

Coordinates

Volume XX, Issue 12, December 2024

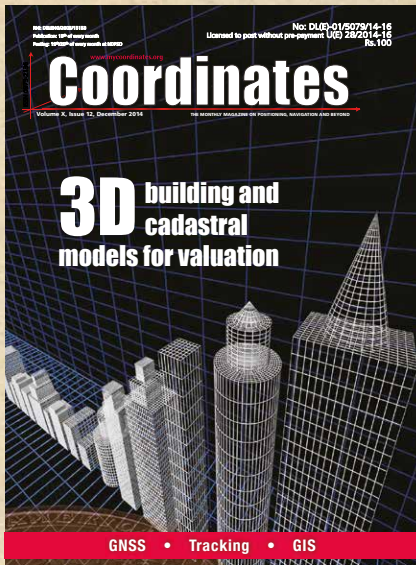
THE MONTHLY MAGAZINE ON POSITIONING, NAVIGATION AND BEYOND

Assessment of climate change impact using Hydrological model and GIS

The hydrological modeling of Ogbunabali floodplain using remote sensing and geographic information techniques

In Coordinates

10 years before...



mycoordinates.org/vol-X-issue-12-December-2014

Tracking ship using INSAT

Chiranjeevi Vivek G

CSIR – Fourth Paradigm Institute, Bangalore, India. Previously worked in National Institute of Ocean Technology, Chennai, India

Sudhakar Tata

National Institute of Ocean Technology, Chennai, India

The tracking of ships using Indian satellite has been successfully implemented, tested and commissioned. The positional information has been exported to an Indian Geoportals, Bhuvan. The system can be used for better tracking in Indian waters using domestic satellite. Commercial decision-making, fleet management and cost control can be improved by using the tracking system. Presently, only one industry provides ship tracking services using various satellites. The developed system is very cost-effective compared to the commercially available vessel tracking services. Ships can be tracked in the vast Indian Ocean region if INSAT-DRT modem is used, since the INSAT-DRT satellite footprint is large.

Combined spatial-temporal filtering for interference mitigation in GNSS receivers

Emrah Tasdemir, Lothar Kurz and Tobias G Noll

Chair of Electrical Engineering and Computer Systems, RWTH Aachen University, Germany

This paper presents a combined spatial-temporal filter for interference mitigation in an antenna-array GNSS receiver. The filter is based on the spatial filter introduced in (Tasdemir, 2013) and extends this by a bank of adaptive FIR-filters in the front. These are used as notch filters and take over the mitigation of narrowband interference by attenuating certain frequencies in the frequency spectrum of the input signal. The adaptation to the interference situation follows a gradient-based power minimization method.

Implementations in planning of public services in Riyadh

Saleh Mohammed Al Saif

Manager of public services planning unit, High Commission for the Development of Arriyadh, (ADA), Saudi Arabia

This plan aims to improve the level of these services in the city, fill the existing gap and identify the future needs of Arriyadh

Semantically rich 3D building and cadastral models for valuation

Umit Isikdag

Beykent Üniversitesi Ayazaga Kampüsü Sarıyer/Istanbul, Turkey
Mike Horhammer, Oracle, USA

Sisi Zlatanova

Delft University of Technology, Faculty of Architecture and the Built Environment, Department OTB, GIS Technology Section, Delft, The Netherlands

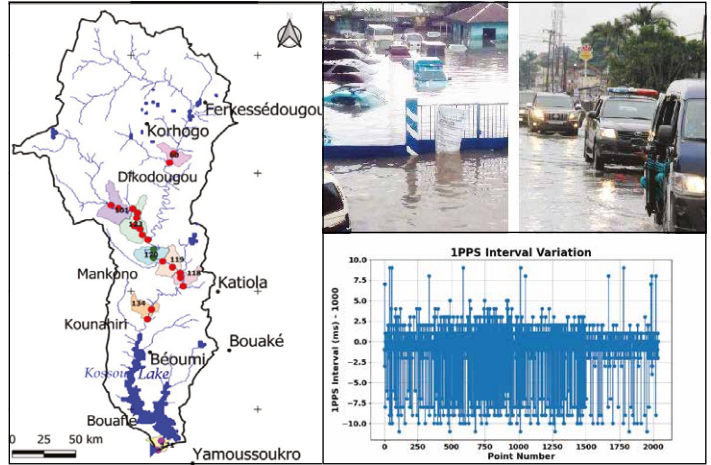
Ruud Kathmann

Member, Management team, Netherlands Council for Real Estate Assessment, The Hague, The Netherlands

Peter van Oosterom

Delft University of Technology, Faculty of Architecture and the Built Environment, Department OTB, GIS Technology Section, Delft, The Netherlands

Despite the fact that analyzed valuation cases in the selected countries are primarily using administrative data for the valuation models, it was argued in this paper that models that use 2D or 3D geometries directly for valuations would have some significant benefits. However, for fair annual valuations, it is clear that the used models and data need to be up-to-date.



In this issue

Coordinates Volume 20, Issue 12, December 2024

Articles

- Using hydrological model and geospatial tool to assess climate change impact on the hydropower potential** KOFFI CLAUDE ALAIN KOUADIO, SIÉLÉ SILUÉ, ERNEST AMOUSSOU, KOUAKOU LAZARE KOUASSI, ARONA DIEDHIOU, TALNAN JEAN HONORÉ COULIBALY, SALOMON OBAHOUNDJÉ, SACRÉ REGIS DIDI AND HOUÉBAGNON SAINT JEAN COULIBALY 5
- Of Imaginary Imageries!** DR MAHAVIR 12
- The hydrological modeling of Ogbunabali floodplain using remote sensing and geographic information techniques** JONAH IYOWUNA BENJAMIN, URIAH JEREMIAH, OKWERE CHIZIANDU ENYINDA AND AKPOMRERE OGHENESUOHWO RUFUS 15
- GNSS Constellation Specific Monthly Analysis Summary: November 2024** NARAYAN DHITAL 26

Columns

- Old Coordinates** 2 **My Coordinates** EDITORIAL 4 **News** IMAGING 30, GNSS 31, UAV 31, INDUSTRY 32
- MARK YOUR CALENDAR 34

This issue has been made possible by the support and good wishes of the following individuals and companies

AKPOMRERE Oghenesuohwo Rufus, Arona Diedhiou, Ernest Amoussou, Houebagnon Saint Jean Coulibaly, JONAH Iyowuna Benjamin, Koffi Claude Alain Kouadio, Kouakou Lazare Kouassi, Narayan Dhital, OKWERE Chiziandu Enyinda, Sacré Regis Didi, Salomon Obahoundjé, Siélé Silué, Talnan Jean Honoré Coulibaly, and URIAH Jeremiah ; SBG System, and many others.

Mailing Address

A 002, Mansara Apartments
C 9, Vasundhara Enclave
Delhi 110 096, India.
Phones +91 11 42153861, 98102 33422, 98107 24567

Email

[information] talktous@mycoordinates.org
[editorial] bal@mycoordinates.org
[advertising] sam@mycoordinates.org
[subscriptions] iwant@mycoordinates.org

Web www.mycoordinates.org

Coordinates is an initiative of CMPL that aims to broaden the scope of positioning, navigation and related technologies. CMPL does not necessarily subscribe to the views expressed by the authors in this magazine and may not be held liable for any losses caused directly or indirectly due to the information provided herein. © CMPL, 2024. Reprinting with permission is encouraged; contact the editor for details.

Annual subscription (12 issues)
[India] Rs.1,800* [Overseas] US\$100*

*Excluding postage and handling charges

Printed and published by Sanjay Malaviya on behalf of Coordinates Media Pvt Ltd

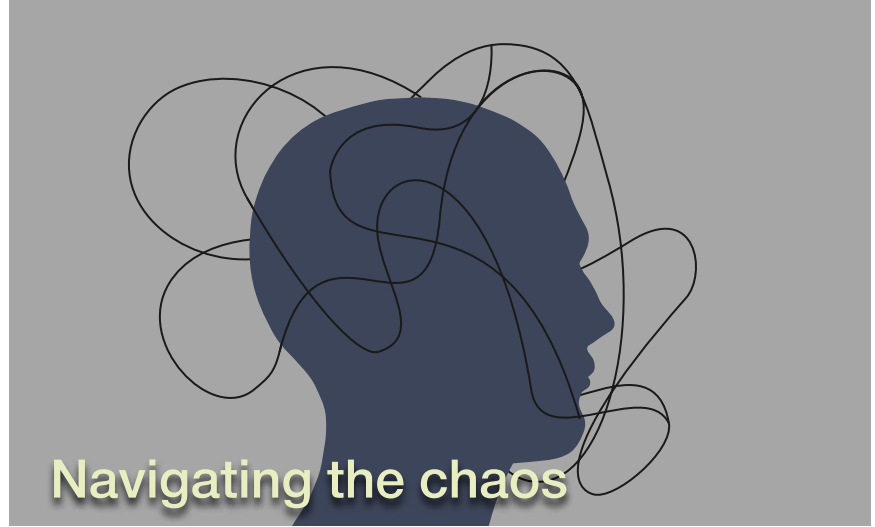
Published at A 002 Mansara Apartments, Vasundhara Enclave, Delhi 110096, India.

Printed at Thomson Press (India) Ltd, Mathura Road, Faridabad, India

Editor Bal Krishna

Owner Coordinates Media Pvt Ltd (CMPL)

This issue of Coordinates is of 36 pages, including cover.



Navigating the chaos

Brain rot—Oxford’s word of the year,

Captures the mental clutter of the digital age,

Where mind lost in data deluge and information overload,

Struggles to stay on track.

When all data is not gold,

And data mines misinformation,

Clarity becomes an asset.

The mind needs clear and precise signals,

To navigate through noisy chaos.

It is less about mapping the world,

More about mapping the world within.

Coordinates wishes a year of peace and prosperity for all in 2025.

Bal Krishna, Editor
bal@mycoordinates.org

ADVISORS Naser El-Sheimy PEng, CRC Professor, Department of Geomatics Engineering, The University of Calgary Canada, George Cho Professor in GIS and the Law, University of Canberra, Australia, Professor Abbas Rajabifard Director, Centre for SDI and Land Administration, University of Melbourne, Australia, Luiz Paulo Souto Fortes PhD Associate Professor, University of State of Rio Janeiro (UERJ), Brazil, John Hannah Professor, School of Surveying, University of Otago, New Zealand

Using hydrological model and geospatial tool to assess climate change impact on the hydropower potential

The purpose of this paper is to adopt a hydrological model combined with a GIS to assess the potential impacts of future Climate Change on the hydropower potential of the White Bandama River watershed in Côte d'Ivoire (West Africa).

Koffi Claude Alain Kouadio

Faculty of Biological Sciences, University of Peleforo Gon Coulibaly, Korhogo, Côte d'Ivoire
African Centre of Excellence on Climate Change, Biodiversity and Sustainable Agriculture, Abidjan, Côte d'Ivoire

Siélé Silué

Faculty of Biological Sciences, University of Peleforo Gon Coulibaly, Korhogo, Côte d'Ivoire

Ernest Amoussou

Department of Geography and Territory Management, University of Parakou, Parakou, Benin

Kouakou Lazare Kouassi

Laboratory of Environmental Sciences and Technologies, University of Jean Lorougnon Guédé, Daloa, Côte d'Ivoire

Arona Diedhiou

Laboratory of Transfer Studies in Hydrology and Environment, University of Grenoble Alpes, Grenoble, France
African Centre of Excellence on Climate Change, Biodiversity and Sustainable Agriculture, Abidjan, Côte d'Ivoire

Talnan Jean Honoré Coulibaly

Laboratory of Geosciences and Environment, University of Nangui Abrogoua, Abidjan, Côte d'Ivoire

Salomon Obahoundjé

African Centre of Excellence on Climate Change, Biodiversity and Sustainable Agriculture, Abidjan, Côte d'Ivoire

Sacré Regis Didi

Laboratory of Environmental Sciences and Technologies, University of Jean Lorougnon Guédé, Daloa, Côte d'Ivoire

Houebagnon Saint Jean Coulibaly

Laboratory of Geosciences and Environment, University of Nangui Abrogoua, Abidjan, Côte d'Ivoire

Abstract

This study was carried out in the White Bandama watershed (WBW) in Côte d'Ivoire (West Africa). The objective is to assess the impacts of future climate change (CC) on the hydropower potential (HPP) of the WBW. The methodology is based on coupling the SWAT (Soil and Water Assessment Tool) hydrological model with the Geographic Information System (GIS) QGIS to assess HPP on streams and evaluate the impacts of future CC on HPP of the watershed. Historical and climate projection data (precipitation, minimum and maximum temperature) for a set of three Regional Climate Models (RCM) from CORDEX-AFRICA (CCCmaCanRCM4, CCLM4-8-17 and REMO 2009) under RCP 4.5 were used. The biases of the ensemble mean were corrected by the Delta change method. The relative change of streamflow discharge and HPP was assessed as the relative difference between the projection periods (2041–2070 and 2071–2100) and the reference period (1976–2005). The results showed a total of 22 future hydropower potential sites in the watershed. These sites were identified, geolocated and classified according to their potential capacity of generation in 82 % as small (1–25 MW potential capacity), 9 % as medium (25–100 MW potential capacity) and 9 % as large (more than 100 MW

potential capacity) hydropower. The climate models' ensemble projected an upward trend for both the annual mean discharge of rivers and HPP of the WBW according to RCP 4.5 for the periods 2041–2070 and 2071–2100. On the annual cycle, the months of August and September will record the highest monthly mean flows between 150 and 200 m³ s⁻¹ while the months from November to April will record low monthly mean flows in the WBW.

1 Introduction

Hydroelectricity (HE) represents the largest source of renewable electricity in the world with a global production of more than 4250 TWh of electricity (IHA, 2022). In West Africa, HE contributes about 40 % of total electricity production (Barbier et al., 2009). In Côte d'Ivoire, HE is the second source of energy production after thermal energy and can contribute to the production of clean electricity with low Greenhouse Gas (GHG) emissions (Kouadio et al., 2020; IEA, 2020). HE could be an essential energy of the future to mitigate climate change (CC). However, there is a duality relationship between hydroelectricity and climate (Kouadio et al., 2022). Although contributing to CC mitigation through its low GHG emission, hydroelectricity can be affected by climate due to changes in the hydrological cycle (Berga, 2016). HE is dependent on climatic parameters (precipitation, temperature, insolation, potential evapotranspiration [PET], etc.) (De Souza Dias et al., 2018). These parameters influence the availability of water resource, the hydropower potential (HPP) and therefore the HE. Previous studies by Amoussou et al. (2012), Kouame et al. (2019) and Kouadio et al. (2020, 2022) have shown that CC can influence the intensity and duration of precipitation as well as river flows. It can also vary the PET. Furthermore, rainfall deficits cause runoff deficits (Savane et al., 2002) and impacts on HE (Kouadio et al., 2020). In the literature, numerous scientific works, in particular authors such as Hamududu and Killingveit

(2012), Grijzen (2014) and, Turner et al. (2017) focused, on the one hand, on the potential impacts of CC on water resources/on hydrology and, on the other hand, on hydropower. All these studies have endeavored to demonstrate that CC has impacts on both water resources and hydroelectric production. Analyzing the impacts of CC on hydrology and HPP in different watersheds in Africa, Yira et al. (2021) and Nonki et al. (2021) proposed a methodology based on the use of a hydrological model and climate model outputs. Thus, this study is a contribution to the establishment of a methodology using hydrological modelling coupled with geospatial analysis to assess the impacts of CC on the HPP in the White Bandama watershed (WBW) in Côte d'Ivoire. The purpose of this paper is to adopt a hydrological model combined with a Geographic Information System (GIS) to assess the potential impacts of future CC on the HPP of the White Bandama River watershed. This article is structured as follows: after the Introduction, which presents the background and objectives of this study, the Materials and Methods section describes the materials and methods used, the main results and discussion are presented in the Results and Discussion section. This manuscript ends with the Conclusion section.

2 Material and methods

2.1 Study area

This study was conducted in the WBW with an area of approximately 32 400 km² (Côte d'Ivoire) (Fig. 1). The WBW extends from the center to the north of Côte d'Ivoire. Its geographic coordinates in the WGS 84 reference vary between 5° and 6°30' in longitude and between 6°30' and 10°30' in latitude. The White Bandama River has its source in the northern part of Côte d'Ivoire between Boundiali and Korhogo, at an altitude of 480 m. The WBW is under the influence of two climates: the Baoulean climate or equatorial climate or attenuated transition with annual precipitations varying on average between 1000 and 1600 mm yr⁻¹ and the sudanian climate or tropical climate of transition with annual precipitations of unimodal distribution varying between 1000 and 1200 mm yr⁻¹ (Goula et al., 2007). The population living on the WBW is estimated ~ 3 000 000 inhabitants (Ivorian Institute of Statistics, 2014). In 1972, one of the major socio-economic assets of Côte d'Ivoire, the Kossou hydroelectric dam was built in this basin, with an installed capacity of 174 MW.

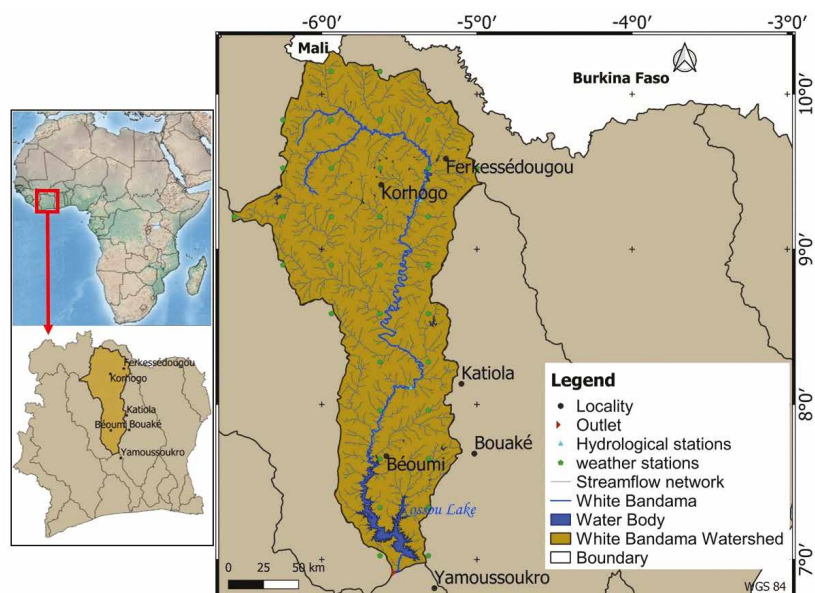


Figure 1. Location of the White Bandama Watershed (WBW).

2.2 Description, data and configuration of the SWAT model

In this study, hydrological modelling was carried out with the SWAT (Soil and Water Assessment Tool) model (<https://swat.tamu.edu/software/>, last access: 17 May 2022) coupled with the QGIS interface (<https://download.qgis.org>, last access: 17 May 2022). The choice of this model is justified by a wide field of applications and use in several relatively recent studies. In addition, coupling facilitates access to variables and parameters. It offers a set of GIS tools for the development, execution and editing of hydrological inputs, and promotes the management of raster, vector and alphanumeric data. SWAT is an agrohydrological model developed by researchers at the Agricultural Research Service (ARS) of the United States Department of Agriculture (USDA) in the 1990s. It is a physically based, spatially distributed, basin-scale hydrological model developed to simulate the impact of land use and management practices on water quantity and quality (surface water and groundwater). A detailed description of the model can be found in the work of Neitsch et al. (2011) and Arnold et al. (2012). The SWAT model simulates the water cycle through the hydrological Eq. (1):

$$SW_t = SW_0 + \sum_{i=1}^t (R_i - Q_{si} - E_i - W_i - Q_{qwi}) \quad (1)$$

With: SW_t : final soil water content (mm), SW_0 : initial soil water content on day (mm), t : time (day), R_i : precipitation of day i (mm), Q_{si} : surface runoff on day i (mm), E_i : potential evapotranspiration on day i (mm), W_i : percolation or infiltration of day i (mm), Q_{qwi} : low water flow or quantity of water returning to the soil of day i (mm).

Several data were needed to configure the model and simulate the flows. The satellite images were obtained by the NASA (National Aeronautics and Space Administration) and NGA (National Geospatial Intelligence Agency) radar surveying mission in 2000. These satellite images are 30 m spatial resolution and are available on the United States Geological Survey (USGS) website

<https://earthexplorer.usgs.gov> (last access: 10 December 2021). In addition, daily re-analysis data of precipitation, temperature (minimum and maximum), relative humidity, solar radiation, wind speed available for a period of 34 years (1980 to 2013) with a resolution of 38 km were used. They are available at <https://globalweather.tamu.edu/> (last access: 10 December 2021; Saha et al., 2014). These reanalysis data collected at a daily time step were aggregated in monthly time step before the simulation of the SWAT model at the monthly time step. The daily hydrometric data observed were collected from the Ivorian direction of human hydraulics (DHH) for the stations of Marabadiassa (1980 to 2013) and Badikaha (1982 to 1989). The model setup also required soil and land cover data in raster form. For this purpose, a soil map of the WBW with a spatial resolution of 1 km provided by the Food and Agriculture Organization of the United Nations (FAO) was used. The WBW land cover map from 2006, with a spatial resolution of 300 m,

was obtained from the ESA website (http://due.esrin.esa.int/page_globcover.php, last access: 10 December 2021; Leroy et al., 2006). PET was computed using the Penman-Monteith equation. The variable storage method developed by Williams (1969) was chosen for the discharge simulation. Runoff was computed using the Curve Number (CN) method. The simulation period was defined from 1980 to 2013 (34 years) with a warming period of 2 years (1980–1981). The configured and calibrated model was used to assess the potential impacts of CC. The model was calibrated from 1982 to 1985 (4 years), and validated from 1986 to 1989 (4 years) at a monthly time step by the coefficient of Nash-Sutcliffe (NS) and the coefficient of determination (R^2).

2.3 Assessment of future climate impacts on hydropower potential

For the assessment of CC impacts, the outputs (precipitation, minimum and maximum temperature) of three

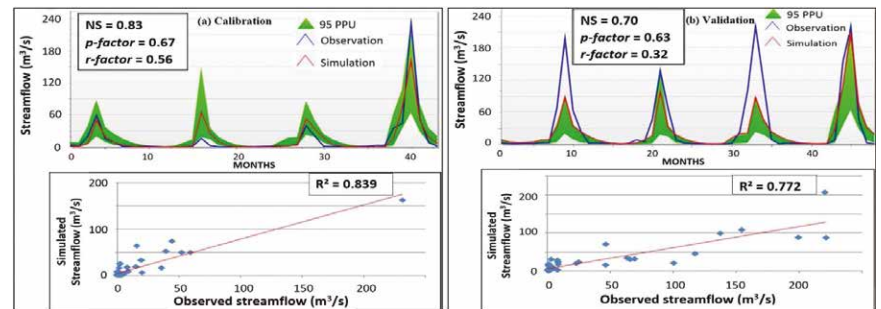


Figure 2. (a) Calibration of the SWAT model of the WBW from 1982 to 1985 (Badikaha station) and (b) Validation of the WBW SWAT model from 1986 to 1989 (Badikaha station). * p-factor: percentage of observed data framed by 95 % prediction uncertainty (95PPU). r-factor: thickness of the 95PPU strip.

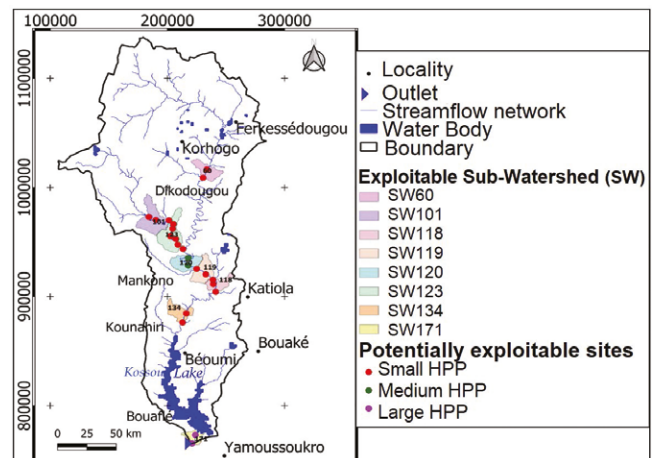


Figure 3. Geospatial distribution of the 22 hydroelectric sites in the WBW.

CORDEX-AFRICA climate models (0.44° resolution) were used: CCCmaCanRCM4, CCLM4-8-17 and REMO 2009. These data were obtained for the RCP 4.5 scenario for the reference period P0 (1976–2005) and the projection periods P1 and P2 respectively (2041–2070) and (2071–2100). In this study, the methodological approach for evaluating the impacts of CC on the HPP is based on a process similar to that used by De Oliveira et al. (2017). Bias correction of the dataset mean of the three climate models was performed by the Delta-Change method (Teutschbein and Seibert, 2012). The HPP was assessed over the reference periods P0 and projection

periods P1 and P2 of the RCP 4.5 by Eq. (2) of Maher and Smith (2001).

$$HPP = \rho g Q \cdot h \quad (2)$$

With: HPP: hydropower potential (W), ρ : density of water (1000 kg m⁻³), g: acceleration due to gravity (m s⁻²): 9.81 m s⁻², Q: flow in (m³ s⁻¹) on the section of the network, h: vertical drop height in meters (m).

The relative change (Δ) characterized by the fluctuations makes it possible to assess the potential CC impacts over the projection periods (2041–2070 and 2071–2100) by Eq. (3).

$$\Delta = \left(\frac{\bar{X}_{proj} - \bar{X}_{ref}}{\bar{X}_{ref}} \right) \times 100 \quad (3)$$

With: Δ : Relative change or fluctuation, \bar{X}_{proj} : Average value of the variable calculated on the projection period \bar{X}_{ref} : Average value of the variable calculated on the reference period.

3 Results and discussion

3.1 Model calibration and validation

The calibration and validation of the SWAT model on the WBW are shown in Fig. 2a and b. The results are illustrated here for the Badikaha hydrological station. The Nash-Sutcliffe (NS) and determination (R^2) coefficients obtained (NS and $R^2 > 0.6$) indicate that there is a very good correlation between the simulated and observed flows. The whole correlation over the calibration period (NS = 0.83 and $R^2 = 0.839$) is much better than that of the validation period (NS = 0.70 and $R^2 = 0.772$). Furthermore, the model underestimated flood peaks. It would be a limit of the SWAT model.

3.2 Evaluation of the HPP in the WBW

The calibrated and validated model was used for the evaluation of the HPP in the basin. Figure 3 presents potentially exploitable hydroelectric sites and their geospatial distribution in the basin. Twenty two sites have been identified, geolocated and classified according to their potential production capacity at 82 % small (potential capacity 1–25 MW), 9 % medium (potential capacity 25–100 MW) and 9 % large (more of 100 MW) hydropower (Table 1). The results show that the WBW has a good potential in small HE. This would be a major asset in the decentralization of electrification in this basin.

3.3 Impacts of future CC on the HPP

The analysis of the impacts of future CC was carried out on the HPP of the 22 sites spread over eight Sub-Watersheds (SW

Table 1. Distribution of HE sites by type.

SW	No. of sites	Generation capacity per HE class (MW)	HE type	Distribution
60	2	[1–25[Small HE	18 sites or 82 %
101	3	[1–25[Small HE	
118	3	[1–25[Small HE	
119	2	[1–25[Small HE	
123	6	[1–25[Small HE	
134	2	[1–25[Small HE	2 sites or 9 %
120	2	[25–100[Medium HE	
171	2	> 100	Large HE	2 sites or 9 %

22

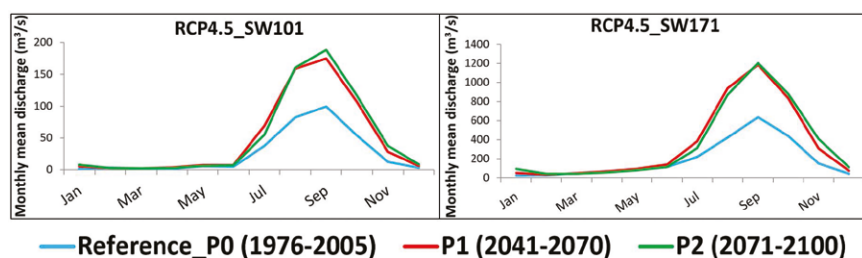


Figure 4. Projected monthly mean discharges of SW101 and 171 under RCP 4.5 of the ensemble mean of the three RCM.

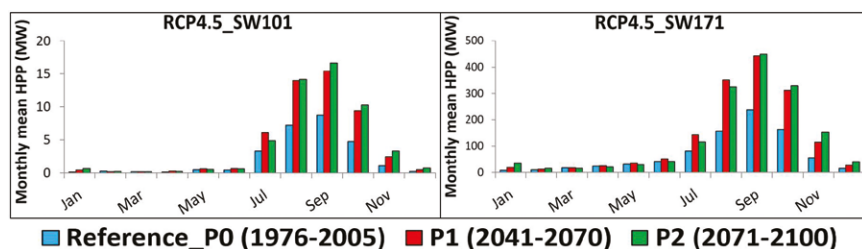


Figure 5. Projected monthly mean HPP of SW 101 and 171 under RCP 4.5 of the ensemble mean of the three RCM.

60, 101, 118, 119, 120, 123, 134 and 171). The relative changes in monthly average flow and HPP for SWs 101 and 171 are shown in Figs. 4 and 5. Compared to the reference period P0, all the climate models project a general upward trend in flows on the eight SWs for the periods P1 and P2 according to the RCP 4.5 scenario. On an annual cycle, flows will increase from July to October. This increase in flows over this period is estimated at a rate of ~ 35 % and 53 % respectively on P1 and P2 for SW 101, and ~ 54 % and 65 % respectively on P1 and P2 for SW 171. Like the discharges, the models project an increase in HPP on all SWs compared to the reference period P0. Furthermore, the results show that SW 171 will register the largest HPP with a monthly average during the months of August and September oscillating between 400 and 500 MW according to the RCP 4.5 scenario. The SW101 will record the lowest HPP with a monthly average maximum of less than 18 MW during these same months.

4 Discussion

The analysis of CC impacts on the HPP used outputs from a set of three CORDEX- Africa climate models (ensemble mean). According to Pandey et al. (2019), the use of a set of models would contribute to the reduction of uncertainties in climate projections. The results of the climate impact analysis project a general upward trend in monthly mean stream flow and HPP on the WBW according to RCP 4.5. This increase in flows on P1 and P2 could be explained, on the one hand, by a resumption of rainfall and, on the other hand, by a degradation of the vegetation cover in the medium and long term. This situation would allow strong flow to the detriment of infiltration, as Amoussou et al. (2012). The degradation or reduction of the vegetation cover would favor strong surface runoff to the detriment of infiltration. In addition, the work of Kling et al. (2016), based on the reference (1998–2014) and future (2046–2065) periods, estimate

that an increase in precipitation in West Africa would be of the order of 1 % to 6.8 %. Moreover, according to the fifth report of the GIEC (2014), an increase in precipitation until 2100 is projected according to the scenario considered. However, these projections remain marked by many uncertainties. For this reason, in this study it would be interesting to consider the general trend marked by a future increase in flows and HPP over the basin for P1 and P2 compared to the reference P0.

In the work of Kouadio et al. (2020), hydrological dynamics was analyzed under CC in the WBW. This study has shown that the Kossou dam plays a role in reducing floods in the watershed. Moreover, the analysis of monthly flows has demonstrated that the flood flow incoming to the Kossou Lake was skimmed ~ 93.7 %

5 Conclusion

The objective of this study was to assess the potential impacts of CC on the HPP of the WBW in Côte d'Ivoire. For this purpose, the SWAT hydrological model combined with geospatial analysis was applied. The potential impacts of CC on the monthly flow and HPP of the basin were analyzed over the projection periods P1 and P2 compared to the reference period P0, under the RCP 4.5 scenario. The analysis of these impacts also focused on eight (8) SWs with twenty two (22) HE sites identified (SW 60, 101, 118, 119, 120, 123, 134 and 171). In comparison with the P0 reference period, a general upward trend in flows and HPP on the WBW was observed. On the annual cycle, the models have projected that the months of August and September will register the highest flows between 150 and 200 m³ s⁻¹ with a high HPP while the months of November through April will register the lowest flows with a low HPP. In addition, an increase in flows and HPP on the 8 SWs for periods P1 and P2 compared to P0 is projected. The models also showed that the SW 171 would have the largest HPP with a monthly

average during the months of August and September oscillating between 400 and 500 MW. In addition, SW 101 will record the lowest HPP with an average monthly maximum of less than 18 MW during these same months. This general increase in flows could however increase the problems of siltation, eutrophication and the risk of flooding in certain areas and for certain activities in this basin. To this end, additional studies should be carried out to better assess these consequences on the basin.

Data availability. The data used in this study is publicly available. The reanalysis data are freely available at <https://globalweather.tamu.edu/> (SWAT, 2021), and the satellite data are available on the USGS website (<https://earthexplorer.usgs.gov>, USGS, 2021) and the ESA website (http://due.esrin.esa.int/page_globcover.php, ESA, 2021). However, the observed data comes from national service databases available upon request.

Author contributions

Conceptualization: KCAK, SS, EA, and AD; Data analysis: KCAK, EA, and AD; Methodology: KCAK, AD, and TJHC; Validation, KCAK, and AD; Drafting of preliminary manuscript: KCAK, SS, and AD; Revision and writing of the final manuscript: KCAK, SS, EA, KLK, AD, TJHC, HSJC, SRD, and SO. The final version of the article was approved by all authors: KCAK, SS, EA, KLK, AD, TJHC, SO, SRD, and HSJC.

Competing interests

The contact author has declared that none of the authors has any competing interests.

Disclaimer. Publisher's note

Copernicus Publications remains neutral with regard to jurisdictional claims in published maps and institutional affiliations.

Special issue statement

This article is part of the special issue “IAHS2022 – Hydrological sciences in the Anthropocene: Variability and change across space, time, extremes, and interfaces”. It is a result of the XIth Scientific Assembly of the International Association of Hydrological Sciences (IAHS 2022), Montpellier, France, 29 May–3 June 2022.

Acknowledgements

The authors would like to thank the organizing committee of the XIth Scientific Assembly of the International Association of Hydrological Sciences in Montpellier 2022. We also thank IAHS through the SYSTA grant for funding the first author to attend this conference and for giving the opportunity to publish this paper. Thanks also to Jean Marie Kileshye Onema and the anonymous reviewer who contributed to improving the quality of this paper.


Review statement. This paper was edited by Christophe Cudennec and reviewed by Jean Marie Kileshye Onema and one anonymous referee.

References

- Amoussou, E., Camberlin, P., and Mahé, G.: Impact de la variabilité climatique et du barrage Nangbéto sur l'hydrologie du système Mono Couffo (Afrique de l'Ouest), *Hydrolog. Sci. J.*, 57, 805–817, <https://doi.org/10.1080/02626667.2011.643799>, 2012.
- Arnold, J. G., Moriasi, D. N., Gassman, P. W., Abbaspour, K. C., White, M. J., Srinivasan, R., Santhi, C., Harmel, R. D., Van Griensven, A., Van Liew, M. W., Kannan, N., and Jha, M. K.: SWAT: Model use, calibration, and validation, *T. ASABE*, 55, 1491–1508, 2012.
- Barbier, B., Yacouba, H., Maïga, A. H., Mahé, G., and Paturel, J.-E.: Le retour des grands investissements hydrauliques en Afrique de l'Ouest: les perspectives et les enjeux, *Geocarrefour*, 84, 31–41, <https://doi.org/10.4000/geocarrefour.7205>, 2009.
- Berga, L.: The Role of Hydropower in Climate Change Mitigation and Adaptation: A Review, *Engineering*, 2, 313–318, <https://doi.org/10.1016/J.ENG.2016.03.004>, 2016.
- De Oliveira, V. A., de Mello, C. R., Viola, M. R., and Srinivasan, R.: Assessment of climate change impacts on streamflow and hydropower potential in the headwater region of the Grande river basin, Southeastern Brazil, *Int. J. Climatol.*, 37, 5005–5023, <https://doi.org/10.1002/joc.5138>, 2017.
- De Souza Dias, V., Pereira da Luz, M., Medero, G. M., and Tarley Ferreira Nascimento, D.: An Overview of Hydropower Reservoirs in Brazil: Current Situation, Future Perspectives and Impacts of Climate Change, *Water*, 10, 592, <https://doi.org/10.3390/w10050592>, 2018.
- ESA (European Space Agency): GlobCover, http://due.esrin.esa.int/page_globcover.php, last access: 10 December 2021.
- GIEC: AR5 Climate Change 2014: Impacts, Adaptation, and Vulnerability. Part B: Regional Aspects, Contribution of Working Group II to the Fifth Assessment Report of the Intergovernmental Panel on Climate Change, edited by: Barros, V. R., Field, C. B., Dokken, D. J., Mastrandrea, M. D., Mach, K. J., Bilir, T. E., Chatterjee, M., Ebi, K. L., Estrada, Y. O., Genova, R. C., Girma, B., Kissel, E. S., Levy, A. N., MacCracken, S., Mastrandrea, P. R., and White, L. L., Cambridge University Press, Cambridge, United Kingdom and New York, NY, USA, 688 pp., <https://www.ipcc.ch/report/ar5/syr/> (last access: 10 January 2022), 2014.
- Goula, B. T. A., Konan, B., Brou, Y. T., Issiaka, S., Fadika, V., and Srohourou, B.: Estimation des pluies exceptionnelles journalières en zone tropicale: cas de la Côte d'Ivoire par comparaison des lois lognormale et de Gumbel, *Hydrolog. Sci. J.*, 52, 49–67, <https://doi.org/10.1623/hysj.52.1.49>, 2007.
- Grijnen, J.: Understanding the impact of climate change on hydropower: the case of Cameroon, World Bank Report No. 87913, Washington, DC, Africa Energy Practice, IBRD/IDA, <https://documents1.worldbank.org/curated/en/243651468010867538/pdf/879130ESW0P1140Box385106B00PUBLIC0.pdf> (last access: 3 May 2022), 2014.
- Hamududu, B. and Killingtveit, A.: Assessing climate change impacts on global hydropower, *Energies*, 5, 305–322, <https://doi.org/10.3390/en5020305>, 2012.
- IEA: Statistics report, Renewables Information: Overview, <https://www.iea.org/reports/renewables-information-overview> (last access: 19 May 2022), 2020.
- IHA: Hydropower Status Report, Sector trends and insights, <https://www.hydropower.org/status-report>, last access: 5 October 2022.
- Ivorian Institute of Statistics: Report of the population statistics from the general population and housing census in Côte d'Ivoire, https://www.ins.ci/documents/RGPH2014_expo_dg.pdf (last access: 3 November 2021), 2014.
- Kling, H., Stanzel, P., and Fuchs, M.: Regional assessment of the hydropower potential of rivers in West Africa, *Enrgy. Proced.*, 97, 286–293, <https://doi.org/10.1016/J.EGYPRO.2016.10.002>, 2016.

- Kouadio, C. A., Kouassi, K. L., Diedhiou, A., Obahoundje, S., Amoussou, E., Kamagate, B., Patuere, J., Coulibaly, T. J. H., Coulibaly, H. S. J. P., Didi, R. S., and Savane, I.: Assessing the Hydropower Potential Using Hydrological Models and Geospatial Tools in the White Bandama Watershed (Côte d'Ivoire, West Africa), *Front. Water*, 4, 844934, <https://doi.org/10.3389/frwa.2022.844934>, 2022.
- Kouadio, K. C. A., Amoussou, E., Coulibaly, T. J. H., Diedhiou, A., Coulibaly, H. S. J. P., Didi, R., and Savane, I.: Analysis of hydrological dynamics and hydropower generation in a West African anthropized watershed in a context of climate change, *Modeling Earth Systems and Environment*, 6, 2197–2214, <https://doi.org/10.1007/s40808-020-00836-4>, 2020.
- Kouame, Y. M., Obahoundje, S., Diedhiou, A., François, B., Amoussou, E., Anquetin, S., Didi, R. S., Kouassi, L. K., N'guessan Bi, V. H., Soro, E. G., and Yao, E. K.: Climate, Land Use and Land Cover Changes in the Bandama Basin (Côte D'Ivoire, West Africa) and Incidences on Hydropower Production of the Kossou Dam, *Land*, 8, 103, <https://doi.org/10.3390/land8070103>, 2019.
- Leroy, M., Bicheron, P., Brockmann, C., Krämer, U., Miras, B., Huc, M., Ninô, F., Defourny, P., Vancutsem, C., Petit, D., Amberg, V., Berthelt, B., Arino, O., and Ranera, F.: GlobCover: a 300 m global land cover product for 2005 using ENVISAT MERIS time series, In *Proceedings of ISPRS Commission VII Mid-Term Symposium: Remote Sensing: from Pixels to Processes*, Enschede (NL), 538–542, http://due.esrin.esa.int/page_globcover.php (last access: 10 December 2021), 2006.
- Maher, P. and Smith, N.: Pico hydro for village power: A practical manual for schemes up to 5 kW in hilly areas, 2nd Edn., Intermediate Technology Publications, 5, Nottingham, UK, https://energypedia.info/images/9/92/Ph_manual_s.pdf (last access: 26 February 2021), 2001.
- Neitsch, S. L., Arnold, J. G., Kiniry, J. R., and Williams, J. R.: Soil and Water Assessment Tool Theoretical Documentation Version 2009, USDAARS GRASSLAND Publication, Texas Water Resources Institute Technical Report No. 406, 77843-2118, Texas, College Station, <https://swat.tamu.edu/media/99192/swat2009-theory.pdf> (last access: 26 February 2021), 2011.
- Nonki, R. M., Lenouo, A., Tchawoua, C., Lennard, C. J., and Amoussou, E.: Impact of climate change on hydropower potential of the Lagdo dam, Benue River Basin, Northern Cameroon, *Proc. IAHS*, 384, 337–342, <https://doi.org/10.5194/piahs-384-337-2021>, 2021.
- Pandey, B. K., Khare, D., Kawasaki, A., and Mishra, P. K.: Climate Change Impact Assessment on Blue and Green Water by Coupling of Representative CMIP5 Climate Models with Physical Based Hydrological Model, *Water Resour. Manage.*, 33, 141–158, <https://doi.org/10.1007/s11269-018-2093-3>, 2019.
- Saha, S., Moorthi, S., Wu, X., Wang, J., Nadiga, S., Tripp, P., Behringer, D., Hou, Y. T., Chuang, H., Iredell, M., Ek, M., Meng, J., Yang, R., Mendez, M.P., van den Dool, H., Zhang, Q., Wang, W., Chen, M., and Becker, E.: The NCEP Climate Forecast System Version 2, *J. Climate*, 27, 2185–2208, <https://doi.org/10.1175/JCLI-D-12-00823.1>, 2014.
- Savane, I., Coulibaly, K. M., and Gioan, P.: Variabilité climatique et ressources en eaux souterraines dans la région semi montagneuse de Man, *Science et changements planétaires/Sécheresse*, 12, 231–237, 2002.
- SWAT (Soil & Water Assessment Tool): CFSR Global Weather Data for SWAT 1979–2014, <https://globalweather.tamu.edu/>, last access: 10 December 2021.
- Teutschbein, C. and Seibert, J.: Bias correction of regional climate model simulations for hydrological climate change impact studies: Review and evaluation of different methods, *J. Hydrology*, 456–457, 12–29, <https://doi.org/10.1016/j.jhydrol.2012.05.052>, 2012.
- Turner, S. W. D., Hejazi, M., Kim, S. H., Clarke, L., and Edmonds, J.: Climate impacts on hydropower and consequences for global electricity supply investment needs, *Energy*, 141, 2081–2090, <https://doi.org/10.1016/j.energy.2017.11.089>, 2017.
- USGS (United States Geological Survey): EarthExplorer, <https://earthexplorer.usgs.gov>, last access: 10 December 2021.
- Williams, J. R.: Flood routing with variable travel time or variable storage coefficients, *T. ASAE*, 12, 100–103, 1969.
- Yira, Y., Mutsindikwa, T. C., Bossa, A. Y., Hounkpè, J., and Salack, S.: Assessing climate change impact on the hydropower potential of the Bamboi catchment (Black Volta, West Africa), *Proc. IAHS*, 384, 349–354, <https://doi.org/10.5194/piahs-384-349-2021>, 2021.
- Proc. IAHS*, 385, 39–45, 2024 <https://doi.org/10.5194/piahs-385-39-2024>

© Author(s) 2023. This work is distributed under the Creative Commons Attribution 4.0 License.

The paper is originally published by Copernicus Publications on behalf of the International Association of Hydrological Sciences. The paper is republished with authors' permission. 

Of Imaginary Imageries!

Appears that Geo-information sciences, Environmental sciences and Social sciences overrule the principles of the grammar of the English language.



Dr Mahavir
Former Professor and
Dean (Academic),
School of Planning
and Architecture,
New Delhi, India

I was going through a paper (Singhal and Gupta, 2024) when the word ‘imaginary’ in the abstract caught my attention. Somehow, the sentence was not making sense, as if a word was missing. This aroused my anxiety and I tried to make sense by going through the whole paper. I became more anxious as the word ‘imaginary’ appeared a few more times, every time leaving a sense of an incomplete sentence. A few examples from the paper are quoted below:

“This allows for the unpacking of a larger urban socio-ecological imaginary being produced.” (p.1); “... which delineates the city’s future waterscape and reveals the environmental imaginary shaping under ...” (p.9); “These fit into the imaginary of Delhi ...” (p.11); “The problem is that they are being carved out of this environmental imaginary.” (p.13); and so on (all quoted from Singhal and Gupta, 2024). The said paper also used the word ‘imaginaries’, presumably to represent the plural of ‘imaginary’ in “... such imaginary has no space for various environmental imaginaries to co-exist.” (Singhal and Gupta, 2024, p.13).

The more I went through the paper, the more I was confused about the usage of the word .. was it to mean ‘image(s)’, ‘imagery’, or an imaginary image, or indeed a different usage of the word ‘imaginary’ with its plural as ‘imaginaries’? Let us set aside this discussion for a while and explore the usage of the word ‘imaginary’.

‘Imaginary’ is something that is created by and exists only in mind (Cambridge Dictionary) or imagination (The Britannica Dictionary). One can have imaginary friends, fears, situations, scenic landscapes, etc. There can be imaginary lines (The Britannica Dictionary) or boundaries. The synonyms could include

made-up, make-believe, non-existent, or fictional (Cambridge Dictionary).

‘Imaginary’ is an adjective (Cambridge Dictionary). An adjective is a word that modifies or describes a noun or pronoun. Adjectives can be used to describe the qualities of someone or something independently or in comparison to something else (Scribbr, 2024). Usage of the adjective ‘imaginary’ without being followed by a noun or pronoun will make the sentence incomplete and will not define the noun or pronoun to which it applies. The usage of ‘imaginary’ without the related noun or pronoun in the above paper (Singhal and Gupta, 2024) thus leaves a void in appreciating the paper fully.

The context of the above paper reminds me of several instances where students and scholars use the word ‘imageries’ (Pratomo, et. al., 2018; Oyedele, 2019) wrongly, most of the time. Imagine, imagination, and imagery ... have their origin in the word ‘image’, which itself is often confused with a picture or a photograph. Until the advancement of computerised image processing, an image was a “generalized mental picture of the exterior physical world that is held by an individual. This image is the product both of immediate sensation and of the memory of past experience, and it is used to interpret information and to guide action” (Lynch, 1959, p.4), implying the ‘imaginary’ aspect. Digital capture of photographs through digital cameras, satellites and (relatively recent) UAVs and further digital processing and production separates photographs (analogue) from images (digital). The product is no longer imaginary (mental, as in Lynch, 1959) but a reality (as in printed form or on a computer screen). What is being depicted can still be imaginary (as in AI). Usage of the word ‘images’ gained more popularity over the words pictures and photographs with the advancement and

mass availability of mobile phones with built-in high-resolution (digital) cameras and digital photo processing. Image processing software used in the fields of satellite remote sensing and medical sciences also popularised the usage of the words 'image' and 'images'. Along came the word 'imagery' to broadly cover the entire field of capturing, processing and producing processed images. It is parallel to the word 'photography', the skill or process of taking photographs (Oxford Languages). While photography is a skill and process, a photograph is a product. Similarly, while imagery is the science and processes, image is a product. The plural of photographs would be 'photographs' (and not photographs), likewise, the plural of image would be 'images' (and not imageries).

Batty and Longley (1994) used the terms 'imagery' and 'images' separately and distinctly to mean 'imagery' as a process (verb) and 'image' as a product (noun). "... and we could complement this display of data with that taken from remotely sensed imagery ..." (Batty and Longley, 1994, p.235) also implies 'imagery' to be a process related to remote sensing. Mahavir (1996) also used the two terms distinctly to mean one as a process and the other as a product. "Satellite imagery refers to the process of capturing visual data of the Earth's surface from satellites orbiting our planet" (Geoimage, 2022). ITC (2008, p.532) describes an 'image' as "... the optical counterpart (pictorial representation) of an object produced by an optical device or an electronic device." At no point, did the classical literature on remote sensing use the term 'imageries' to

mean several images. "A plural verb does not have an s added to it, such as write, play, run, and uses forms such as are, were, have and do" (Good English Movement).

In the non-photographic systems, Aronoff (1993) defined an image as created by light-sensitive detectors that produce electrical signals proportional to the brightness of the light energy. "In physical form, a digital image is a two-dimensional array of small areas called pixels ... that correspond spatially to relatively small ground areas ..." (Avery and Berlin, 1985, p.452). Usage of the term 'image(s)' in the above examples illustrates it to be a product, a noun.

Imagine for a moment, that the intended word in the above-quoted paper (Singhal and Gupta, 2024) was 'imagery'. Let us try replacing the word 'imaginary' with 'imagery' and 'imaginaries' with 'imageries' and see if it makes sense:

"This allows for the unpacking of a larger urban socio-ecological imaginary imagery being produced."; "... which delineates the city's future waterscape and reveals the environmental imaginary imagery shaping under ..."; "These fit into the imaginary imagery of Delhi ..."; "... such imaginary imagery has no space for various environmental imaginaries imageries to co-exist."; "The problem is that they are being carved out of this environmental imaginary imagery."; and so on (all originally from Singhal and Gupta, 2024, editing added).

This began making some sense ... yet not fully comprehensible, 'imagery'

being a process (verb) and 'imageries' not acceptable as a plural of a verb. The Concise Oxford Dictionary (2000, p.708) describes 'imagery' as "(noun) ... visual images collectively". Now if imagery itself is plural, there can not be 'imageries'. The above paper further quotes a paper by Zimmer, Véron and Cornea (2020) with the title "Urban ponds, environmental imaginaries and (Un)commoning: ...", arousing curiosity about whether 'environmental imaginaries' is an acceptable term. Yes, indeed 'environmental imaginary' (and imaginaries) appear to be accepted terms (Nesbitt and Weiner, 2001; Helliwell, Raman and Morris, 2020) which itself has origins in the concept of 'spatial imaginary' developed by Peet and Watts (1993). With this understanding, the usage of the words 'imaginary' and 'imaginaries' in the above paper becomes justified in the context of socio-ecology and environment. Similarly, although 'imagery' in the context of remote sensing also seems acceptable as a noun, 'imageries' as its plural has not gained popularity yet. ITC (2008, p.534) avoided using the word 'imagery'.

Let us examine the sequence from 'image' to 'imaginaries' from the English language viewpoint. 'Image' (noun; verb; plural images) leads to 'imagine' (transitive verb) and 'imagination' (intransitive verb); leading to 'imagery' (noun in literary sense; process-verb in the context of remote sensing) (Merriam-Webster Dictionary). Although in my opinion, 'imagery' is a process and hence a verb. 'Imaginary' is labelled as an adjective (Merriam-Webster Dictionary). However, the word 'imaginaries' did not find a place in this dictionary. 'Imageries' was shown as a plural of 'imagery' but examples of sentence formation with 'imageries' were not provided.

Appears that Geo-information sciences, Environmental sciences and Social sciences overrule the principles of the grammar of the English language. An adjective becomes a noun, and a noun can have a plural. With popular use, nouns can become verbs, e.g. PayTM

Let us examine the sequence from 'image' to 'imaginaries' from the English language viewpoint. 'Image' (noun; verb; plural images) leads to 'imagine' (transitive verb) and 'imagination' (intransitive verb); leading to 'imagery' (noun in literary sense; process-verb in the context of remote sensing) (Merriam-Webster Dictionary)

karo and Google it; and verbs or adverbs can become nouns and can have plural, e.g. ‘imageries’ and ‘imaginaries’. ‘Imagination’ has been dropped out somewhere in the process. After all, English is a language of exceptions.

References:

Aronoff, S. (1993) *Geographic Information Systems: A Management Perspective*; WDL Publications, Ottawa, pp. 47-102

Avery, T. E. and Berlin, G. L. (1985) *Interpretation of Aerial Photographs*, Macmillan, New York, ISBN 0-02-305030-6

Batty, M. and Longley, P. (1994) *Fractal Cities: A Geometry of Form and Function*, Academic Press, London

Cambridge Dictionary

<https://dictionary.cambridge.org/dictionary/english/imaginary>

Geoimage

<https://geoimage.com.au/blog/what-satellite-imagery#:~:text=Satellite%20imagery%20refers%20to%20the,back%20to%20Earth%20for%20analysis>

Good English Movement

<https://www.languagecouncils.sg/goodenglish/resources/grammar-rules/subject-verb-agreement#:~:text=How%20do%20you%20recognise%20a,E.g.>

Helliwell, R., Raman, S., and Morris, C. (2021) Environmental imaginaries and the environmental sciences of antimicrobial resistance. *Environment and Planning E: Nature and Space*, 4(4), 1346-1368.

<https://doi.org/10.1177/2514848620950752>

ITC (2008) *Principles of Remote Sensing: An Introductory Text Book*, (Tempfli, K., Kerle, N., Huurneman, G. C. and Janssen, L. (eds.)), ITC, Enschede, The Netherlands

https://webapps.itc.utwente.nl/librarywww/papers_2009/general/principlesremotesensing.pdf

Lynch, K. (1959) *Image of the City*, The MIT Press, Massachusetts

Mahavir (1996) *Modelling Settlement Patterns for Metropolitan Regions: Inputs from Remote Sensing*, ITC (Publication No. 35), Enschede (ISBN 90-6164-117-9)

Merriam-Webster Dictionary

<https://www.merriam-webster.com/dictionary/image#:~:text=%3A%20a%20visual%20representation%20of%20something,a%20television%20or%20computer%20screen>

Nesbitt, J. T. and Daniel Weiner, D. (2001) Conflicting environmental imaginaries and the politics of nature in Central Appalachia, *Geoforum*, Volume 32, Issue 3, Pages 333-349, ISSN 0016-7185

<https://www.sciencedirect.com/science/article/pii/S0016718500000476>

Oxford Languages

https://www.google.com/search?q=photography+definition&sca_esv=e936ada1b37f2909&rlz=1C1CHBF_enIN757IN757&sxsrf=ADLYWIIlVn9HVGP1MFUNKAT3Ep2nCJ984w%3A1730389916524&ei=nKcjZ7LZH_vVseMP4_eA8QY&ved=0ahUKEWiy17Di_LiJAX7amwGHeM7IG4Q4dUDCA8&uact=5&oq=photography+definition&gs_l=lp=Egxn3Mtd2l6LXNlcnAiFnBob3RvZ3JhcGh5IGRlZmluaXRpb24yCxAAGIAEGJECGIoFMgUQABiABDIFEAAygAQyBRAA GIAEMgUQABiABDIFEAAygAQyBR AAGIAEMgUQABiABDILEAAygAQY hgMYig UyCxAAGIAEGIYDGIoFSJIq UMg TWIYmcAF4AJABAJgBlgGgAeEL qgEEMC4xMrgBA8gBAPgBAZg CDKAC kQvCAgoQABiwAxj WBBh HwgINEAAYs AMY1gQYRxjJ A8ICDhAAGIAEGLADGJIDGIoFwg IOEAAygAQYkQIYsQMYig XCAgoQABiABB gCGMsBwg INEAAygAQYk QIYigUYC sICCxAA GIAEGLEDGIMBwg IFEC4YgASYAw CIBgGQBqgSBwQxLjExoAeD WQ&scient=gws-wiz-serp

Oyedede, A. A. (2019) Use of remote sensing and GIS techniques for groundwater exploration in the basement complex terrain of AdoEkiti, SW Nigeria, *Applied Water Science* (2019) 9:51

<https://doi.org/10.1007/s13201-019-0917-9>

Peet, R. and Watts, M. (1993) Introduction: development theory and environment in an age of market triumphalism. *Economic Geography*, 69(3): 227-253

Pratomo, J., Kuffer, M., Kohli, D. and Martinez, J. (2018). Application of the trajectory error matrix for assessing the temporal transferability of OBIA for slum detection. *European Journal of Remote Sensing*. 51. 838-849. 10.1080/22797254.2018.1496798.

Scribbr (2024)

<https://www.scribbr.com/parts-of-speech/adjectives/>

Singhal S. and Gupta M. (2024) Critically analyzing nature-based solutions: A political ecology framework of planning for the Yamuna River floodplains, Delhi, *Journal of Urban Affairs*, DOI: 10.1080/07352166.2024.2413587

<https://doi.org/10.1080/07352166.2024.2413587>

The Britannica Dictionary

<https://www.britannica.com/dictionary/imaginary>

The Concise Oxford Dictionary (2000), Oxford University Press, New York

Zimmer, A., Véron, R., and Cornea, N. L. (2020) Urban ponds, environmental imaginaries and (Un)commoning: An urban political ecology of the pondscape in a small city in Gujarat, India. *Water Alternatives*, 13(2)

www.wateralternatives.org 

The hydrological modeling of Ogbunabali floodplain using remote sensing and geographic information techniques

The study aims to determine the floodplain hydraulic and hydrological spatial pattern using digital elevation models (DEMs) from topographic survey data.



JONAH Iyowuna Benjamin

Department of Surveying & Geomatics, Rivers State University, Port Harcourt, Nigeria.

URIAH Jeremiah

Office of the Surveyor General, Rivers State, Moscow Road, Port Harcourt, Nigeria.

OKWERE Chiziandu Enyinda

Department of Surveying & Geomatics, Rivers State University, Port Harcourt, Nigeria.

AKPOMRERE Oghenesuohwo Rufus

Department of Surveying and Geoinformatics, Delta State University of Science and Technology, Ozoro, Delta State, Nigeria.

Abstract

Floodplain is a natural ecosystem that has both negative and positive effects on man. It provides land for development, transportation, recreation, agriculture, and hydro power generation. The negative effects are those associated with urban flooding when the land is inundated by water from the rivers, streams, creeks, runoff etc. These effects enable floodplains management programmes to be put in place by the Federal, State, and Local authorities in many countries of the world, mostly, the developed nations. This study was focused on the hydrology and hydraulic modeling and the development of digital database of floodplain of Ogbunabali Port Harcourt, Rivers State, Nigeria. The software used was ESRI's ArcGIS 10.1 and SURFER 10 and the dataset was the topographic survey data obtained at 30m interval and SPOT image with 2.5m x 2.5m spatial resolution. The data was downloaded from total station and saved in excel spreadsheet in xyz coordinates. The elevation data was used to model contour, slope, Triangular Irregular Network, flow direction and flow accumulation which depicted the hydraulic pattern of the floodplain. The hydraulic characteristics of the models were the same and showed that flows came from high gradient (steep slope) to the lower gradient (gentle slope). Similarly, the floodplain digital database consists

of four land use/ land cover which were water body, dumpsite, nypa palm, and built-up area. The total built-up area was 4.413ha, dumpsite 0.626ha, nypa palm 16.583ha, and water body 21.324ha. The database is necessary for the estimation of flood rate damage. High resolution satellite images and 2D floodplain software was used to map all floodplains in Port Harcourt for flood disaster management. In conclusion, the digital database of all floodplains in Port Harcourt City should be developed for the effective management of flood disaster in the city.

1. Introduction

Floodplain according to (FEMA 480, 2005) is defined as any land area susceptible to being inundated by flood waters from any source. The source of floodplain water may be rivers, streams, creeks, lagoons, drainage systems, and runoff water from urban areas. Floodplain has been a major characteristic of most coastal communities with tributaries from the main Atlantic Ocean. Most settlements (city, town, village and hamlet) situated along water channels, creeks, lagoons, and river estuaries in the Niger Delta region. Floodplain may vary in areal extent from one location to another and may vary in term of biodiversities abundance. Generally, identify as a dry area adjacent to wetlands, low lying areas with poor

drainage capability, and small water pond (Department of Natural Resources, 2006). It is formed by deposit of lateral and vertical accretion (Wolman and Leopold, 1957). In addition, materials deposited in floodplain are eroded from upland areas of the drainage basin and from overbank flow.

Floodplain is one of the fertile ecosystems and contain cultural and natural resources that have values to the society. Its functions are enormous and include agricultural activities, water supply, hydropower development, aesthetic beauty, and site for transportation routes (Task Force on the Natural and Beneficial Function of the Floodplain, 2002). It also serves as route for discharge of excess water, and a suitable site for human infrastructural development (Association of Floodplain Managers, 2008). Floodplains also provide groundwater recharge, filter sediment and contaminants, recreational site, and habitat for flora and fauna (West Virginia Quick Guide, 2009). However, most of these functions are gradually degraded due to anthropogenic activities such as mining, intensive agricultural activities, and infrastructural development.

Floodplains a hydrologically important, environmentally sensitive and ecologically productive area is supported with articulated management plan to ensure full utilization of its potential. In Unites States, floodplain management was promulgated by the passage of the National Flood Insurance Act of 1968 (Lynn, 2009). The Act established National Flood Insurance Program (NFIP) administered by the Federal Emergency Management Agency (FEMA). Floodplains management outline regulatory framework for the use, mapping, mitigation, and administration of floodplain areas. Floodplains management is an intergovernmental approach involving the federal, state, and local authority to achieve the stated goals.

Floodplains management is best achieved from detail base map depicting all features in the area and a topographic data to delineate hydrology and hydraulic characteristics of the area. The base map is produced from the horizontal

coordinates obtained from field survey and are used to depict streets, railway lines, stream networks, settlements, and agricultural lands and others features located in the floodplain. Mapping of floodplains may be carried out using conventional survey methods or through aerial photography. The topographic data models the hydrology and hydraulic (H & H) pattern of floodplains which may be used in the determination of flood discharge and frequency, and flood elevation and floodway. Floodplains modeling can be carried out using 1D (HEC-RAS, 2016) and 2D (DHI, 2007) software packages.

This study used DEM from topographic survey to model the hydrology of Ogbunabali floodplain and geographic information systems defined by (Charles and Paul, 2008) as a system of hardware, software, data and organizational structure for collecting, storing, manipulating, and spatially analyzing georeferenced data, and displaying the information resulting from these processes using map.

Floodplains encroachments by human activities are responsible for flash flood in urban areas (FEMA 480, 2005). Floodplains channels may be block by solid waste generated from residential, industrial, and commercial areas. The case is not different from Port Harcourt City where floodplains

channels has been completely covered by solid waste like bottles, plastics, metal objects, papers from schools and factories etc. These humans induce activities on floodplain has been responsible for flood cases in the city. For example, the 2017 flood in some parts of Port Harcourt City causing lost of valuable properties in millions of naira is a good example. The flood affected the office of the Federal Road Safety Commission (FRSC) along Port Harcourt / Aba expressway and other public and private residence in D/Line, Nkpogu, Diobu and Borokiri (Leadership News Paper, July 29 2017). The FRSC office is situated within buffer radius of 30m from the Ntawogba creek. The flood was caused by the blockage of Nwaja and Ntawogba (two major creeks that traverse Port Harcourt City) creeks (Vanguard News Paper, July 24 2017) which resulted to the dumping of solid waste in the creeks according to press release by the Rivers State Waste Management Agency (RIWAMA) boss Brother Felix Obuah. In providing solutions to the problems, this study was carried out using topographic data to model the hydraulic and hydrology of Ogbunabali floodplain and to create an inventory of all features in the area that will guarantee effective floodplain mapping and management.

The study is structured to achieve the following objectives: (i) to determine the



Figure 1: Flooded FRSC office along PH/ Aba expressway. Source: Leadership New Paper, July 29, 2017.

floodplain hydraulic and hydrological spatial pattern using digital elevation models (DEMs) from topographic survey data. (ii) to develop digital floodplain base map (DFBM) of the study area.

1.2 Justification of the Study

The creation of digital database of Ogbunabali floodplain will further advance the awareness of flood impact on properties in the area. Also, the floodplain base map will assist policy makers to provide up to date reports on the extent and damage cause due to flooding. The base map will assist government agencies in identifying flood risk and vulnerable areas based on the floodplain hydrological and hydraulic characteristics.

Several researchers have used different approach in floodplain study with emphases on flood risk zone and vulnerability mapping. (Samarasinghe et al, 2010) used HEC-HMS and HEC-RAS GIS software and remote sensing data to validate flood information forecast, planning and management in Kalu-Ganga River basin, Sri Lanka. The dataset used for the study include; satellite image data, topographic data, hydro-metrological data, and census data. Also, (Lawal et al, 2014) used Minimum Distance Algorithm to develop the extent of flood and compared their effect in flood generation in the state of Perlis, Malaysia. Datasets applied are geological map, topographic map, and SPOT image and these data were processed using GIS software. The study concluded that correlation exist between extracted model and the flood factors. (Bera et al, 2012) used Landsat ETM+, TM, LISS-111, STRM, geological map, climatic data, soil map, groundwater data, rainfall data, and population datasets and ERDAS IMAGINE 9.2, ArcGIS 9.2, and PCI Geomatica-9.1 software to generate flood risk and vulnerability map of Mongalkote block in Eastern India. The study identified five vulnerable flood areas in the study area. Similarly, (Muhammad and Iyortim, 2013) study the middle course of River Kaduna, Nigeria flood that have claimed several lives and properties using high resolution image, field interview

observation, and DEM data. The flood vulnerable areas were model using ArcGIS software and the results overlay on image to show affected properties.

The reviews above from various researchers focused on mapping vulnerable areas and much has not been done in knowing floodplains hydraulic pattern which is main input in the management process of floodplains. In this study the emphasis is on modeling hydrology and hydraulic nature of Ogbunabali, Port Harcourt floodplain using elevation data obtained from field survey, and ArcGIS 10.1 was utilized to perform the modeling. The study also, develop digital floodplain database from satellite image to aid its management.

II. Literature review

The section discussed the general methods of delineating floodplains and the available methods of acquiring digital terrain models (DEMs) for studying floodplains hydrology and hydraulic patterns.

2.1 Methods of Generating Floodplain Map

2.1.1 Conventional Survey Method

Floodplain may be map using traditional survey methods to obtained planimetric points defining the area. The traditional survey method involves the use of Theodolite or Total station to carry out measurements of details within floodplains. The Theodolite or Total station may be 1” or 2” instrument to approve the measurement accuracy. The observed data may be recorded directly in the field sheets or downloaded from the memory in the case of Total station. Conventional floodplain mapping methods may be suitable for small area and less difficult terrain. According to (FEMA 480, 2005) floodplain maps are used for the regulating of new flood prone areas, insurance policies, and granting of loan by the lenders and federal agencies.

2.1.2 Remote Sensing Method

With the advancement in technology, remote sensing is now used in the mapping of floodplains because of large area coverage capability and in accessing inaccessible parts of the globe. Remote sensing data depending on altitude may be high, medium, and low spatial resolution. According to (Dano et al, 2011) satellite imageries for floodplain delineation are categories as optical sensor example Landsat image, and microwave sensor example Radar satellite image. Landsat image is mostly used in floodplain mapping because they can be downloaded free-of-charge from its website in any part of the globe. Landsat satellite was launched into orbit on July 23, 1972 (Anji 2008) for environmental studies.

Floodplain can also be mapped using SPOT image (Lawal et al, 2014). SPOT image is a 2.5m x 2.5m spatial resolution image launched by France in 22 February, 1986 (Richards and Xiuping, 2006). Others high spatial resolution image for floodplain mapping includes Quick Bird, and IKONOS with 0.61m and 1m spatial resolution respectively. High cost of these images has prevented its use for floodplains mapping.

Remote sensing data can be used to generate different types of floodplain maps such as Flood Hazard Boundary Map (FHBM), and Flood Insurance Rate Map (FIRM) (FEMA 480, 2005). The various maps are useful in floodplain management and planning.

2.2 Sources of data for floodplain Hydrological modeling

2.2.1 DEM from traditional Survey technique

Traditional surveying technique is the oldest method of acquiring digital elevation model (DEM) of the earth’s surface. The traditional survey techniques of observing DEM includes the used of differential global positioning system (DGPS), leveling instrument, total station and theodolite (Zhilin et al, 2005). The

used of theodolite instrument in acquiring DEM is now in extinction and obsolete in the field of spatial information science and surveying. Total station instrument is capable of measuring x, y, z of points on the earth's surface using observed distance, bearing, and the control coordinates.

Today, DGPS is being used in acquiring DEM data accurately over an area and gradually replacing total station and theodolite. DGPS works using the principle of trilateration to fix its position by making measurement to minimum of four satellites orbiting the earth.

Traditional DEM is created by observing regularly or irregularly spaced horizontal coordinates (x, y) and vertical coordinate (z) points on the earth's surface. The grid interval of the observation represents spatial resolution of the DEM data. (Heywood et al, 2006) stated that traditional survey method of obtaining elevation data is more accuracy since the observations are connected to a known control and covered relatively small area.

2.2.2 DEM from photogrammetric data

Photogrammetry is another method of acquiring digital elevation model (DEM) of surface locations. Punmia et al., (2005) defined photogrammetry as the science and art of obtaining accurate measurements by use of photographs taken from specific altitude for the purpose of constructing topographic maps, classification of soil, geological mapping, and for military operations. This field of study started in the 19th century by Aime Laussedat, an officer in the Engineering Corps of the French Army and is being regarded as the father of photogrammetry (Zhilin et al, 2005). In 1849 Laussedat justified the use of photograph to prepare topographic map and this might mark the beginning of application of photogrammetry in topographic mapping.

2.2.3 DEM from LiDAR data

LiDAR (also called LADAR or laser altimetry) is an acronym for light detection and ranging (NOAA, 2012). LiDAR is an airborne system for large area coverage

and some are used as ground-based stationary and mobile platforms for data collections. It is an elevation data source fitted with an active laser pulse which enhanced its efficiency in working day and night (Hiremath and Kodge 2010, www.aerometric.com/ LiDAR). LiDAR data are mostly collected at night and under clear weather conditions. It operated in the near-infrared region of the electromagnetic spectrum, while the bathymetric LiDAR operated in the green laser wavelength with greater penetration of water and the ability to detect bottom features. Unlike other remote sensing systems, LiDAR records ground elevation in thick vegetation areas through the canopy holes. The absolute accuracy of LiDAR system ranges from 10cm to 20cm for most recent data and 15cm to 30cm for older data LiDAR (NOAA, 2012).

LiDAR computes x, y, z (eastings, northings and height) of target features using time difference between transmitted and return laser pulse, the transmitted angle of the pulse, and location of the sensor above the earth surface. The horizontal resolution of points spacing is between 1m to 2m but higher LiDAR may have eight points per 1m coverage.

LiDAR system has been used in different application areas. It is used in the mapping of North Carolina floodplain (North Carolina Cooperating Technical State, 2003), delineation of vulnerable areas to sea level fluctuation (Dean, 2009), and in shoreline extraction (Lee et al, 2010). Others applications areas includes forestry and infrastructure inventories (Jay, 2010). LiDAR data can be used in the following surface modeling such as; contour map, slope model, triangular irregular network, cross section determination, flow direction and accumulation models, watershed delineation to mention a few.

III. Methodology

The chapter focused on two main sub-headings which is (a) identification of dataset and software used for the study and (b) the data processing techniques adopted. The dataset and software were

set of data (primary or secondary) and software (vector or raster) required for the study. While data processing involves all the processing methods such as digitizing, surface modeling and plotting of maps carried out in the study. Data processing was an office-based operation. The methodology was designed to achieve all the stated objectives of the study.

3.1 Dataset and Software

The study was carried out using elevation data at 25m grid interval obtained from Total station traverse. Secondly, high resolution SPOT satellite image clipped from Google Earth with a spatial resolution of 2.5m x 2.5m was used to digitize features within the study area floodplain.

Similarly, the following software were used to facilitate this study and they are;

- a. ESRI's ArcGIS 10.1 vector base GIS software was used to digitized the features in the study area and creation of geodatabase, hydraulic modeling of the floodplain and compilation of maps.
- b. SURFER 10 was used to generate additional digital terrain model (DTM) such as wireframe and flow direction models which are significance in the interpretation of floodplain hydrology.

The data processing ability of software was supported by computer application programs for specific task.

3.1.1 Control Establishment

Three control points were established on stable locations at close proximity to the project site. The control points were established such that they are intervisible during observations. The control points were established and observed using Promark 3 DGPS in static mode. The observations were taken for 30mins per station for accurate position fixing.

3.1.2 Total Station Traversing

Traversing from the established control points was carried out in other

to determine eastings, northings and elevation (X, Y, Z) of the ground points (Kavanagh, 2010) of the study area. The observations were taken at grid interval of 25m throughout the study location. The observations were taken using Leica 805 Total station instrument and its accessories. Prior to this observation, the Total station was calibrated at SHELL calibration base and was found to satisfy the requirement for this project. The observations were recorded directly in the instrument and downloaded using Leica Survey Office (Leica instrument downloading software). The observations were exported to excel spread sheet for further analysis of floodplain hydraulic modeling.

3.2 Data Processing

3.2.1 Generation of Triangular Irregular Network (TIN)

Triangular irregular network (TIN) is a digital elevation model (Sulebak, 2000) and is one of the methods of hydraulic modeling of floodplain. TIN model produced a network of triangular surfaces based on interpolated points with the vertices representing peaks, depressions and passes, and the triangular edges represents ridges and valleys (Heywood et al, 2006). TIN model can be generated using different software, for example, (Muhammad, 2006) used Global Mapper software but in this study ArcGIS 10.1 was used to generate TIN.

TIN model was produced from the points data download from Total station and saved in MS excel in eastings, northings and elevation column. The data was added to ArcGIS window using add data button and was later converted to shape file format. By enabling the 3D Analyst tools from the Arc Toolbox, create TIN module was double click and the shape file was selected as input feature class. The mass points were selected as the surface feature types to represents the geometry of the imported points. The output TIN was generated using default nine (9) classes of equal interval to represents the floodplain terrain. The TIN operation screen print from ArcGIS window is shown in figure 2.

3.2.2 Slope Model

Slope model is very useful in hydraulic modeling of floodplain. It describes the topography of the study area from the interpolated points. The TIN created above was converted to raster by double clicking TIN to Raster from the 3D Analyst Tools. The slope model was generated by double clicking slope from the raster surface module and the converted TIN to raster selected as input file. The output file was generated using degree of slope as output measurement with nine (9) classes of equal interval. The screen print of slope generation dialogue box from ArcGIS was shown in figure 2.

3.2.3 Contour Model

Contour line joins all points of equal elevation and perhaps one of the traditional applications of digital terrain models

Table 1: Coordinate Listing of Control Stations.

STATION	EASTINGS	NORTHINGS	ELEVATION (m)
TBM1	280194.032	530231.983	5.01
TBM2	280248.295	530250.647	5.24
TBM3	280063.270	530178.334	4.97

(DTMs). It is based on interpolation principle (Zhilin et al, 2005) where values are generated at unknown locations within the study area. Contour models are used to delineate linear features such as banks and channel thalweg and point feature such as hills and sinks in the floodplain.

It is generated by double clicking contour from the raster surface module in the 3D Analyst Tools. In the dialogue box the raster model created earlier represents input raster and a contour interval of 0.10m was specified to produce contour model. Contour generation dialogue box is shown in figure 3.

3.2.4 Flow Direction Model

The flow direction is a digital terrain model used in floodplain hydraulic modeling. It shows the direction of surface

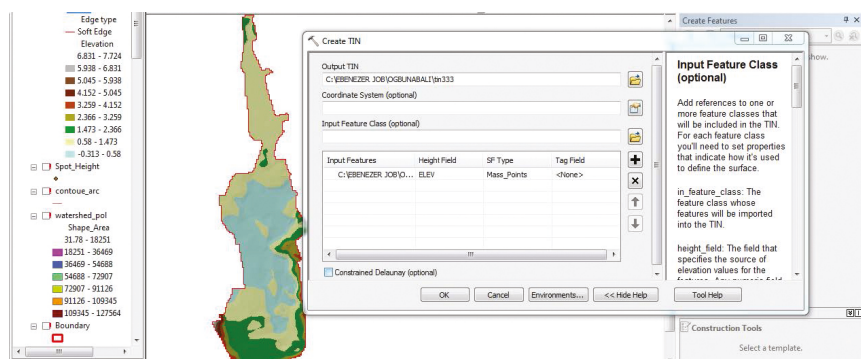


Figure 2: Screen print of TIN creation dialogue box.

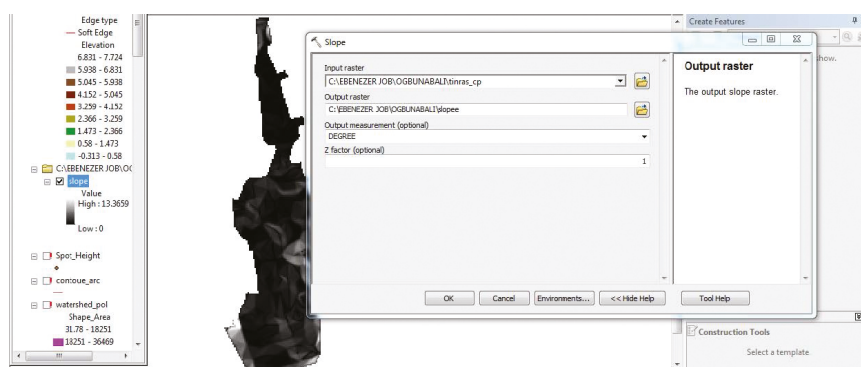


Figure 2: Screen print of slope generation dialogue box.

and groundwater flow within floodplain. Flow direction was generated using blank grid file in SURFER 10 software.

3.2.5 Creation of Floodplain Geo-database

Floodplain mapping and management is facilitated through creation of geo-database for the feature class. It is a relational database storing floodplain spatial and attributes data (Francisco et al, 2011). Geo-database is managed by the database management system (DBMS) (Otto and Rolf 2009) and of different types. The floodplain geo-database according to (Lynn, 2009) can provide the following advantages:

- Removal of redundancy
- Concurrency control
- Transferability
- And data standardization.

The geo-database was created in ArcGIS 10.1 by digitizing features in the floodplain study area. In this floodplain, four features' types such as water body, built-up, nypa palm, and dumpsite were digitized from the SPOT satellite image. However, the digitization from image was validated by the traverse observation that was used to produce the final output map.

3.3 Study Area

Ogunabali floodplain in Port Harcourt local government Area, Rivers State, Nigeria is located on longitude 279745mE – 280246mE and latitude 530161mN – 531922mN in the WGS-1984, UTM Zone 32N coordinates system. The floodplain has a total area of 42.943ha and perimeter of 4657.99m and it is narrow in the north and wider in the southern part. It is bounded by Elekahia in the north, Nkpogu in the east, Amadi-ama in the south, and Ogunabali in the west. The floodplain is tributary of Amadi-ama River (salt and tidal river) that flows to and from Nwaja creek. The creek (Nwaja) has been a source of flash flooding in the area over the years as result of channel blockage. The floodplain is currently used in some part as dumpsites, and building of slum settlements along water course. The remaining parts are covered by water body and Nypa palm vegetation.

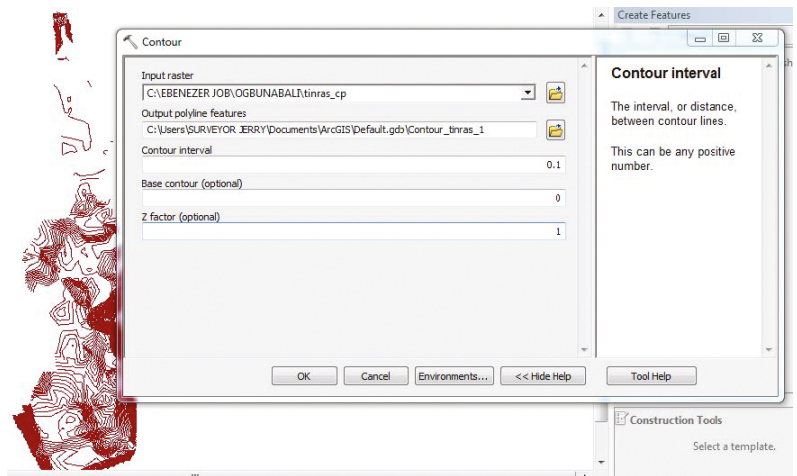


Figure 3: Screen print of contour generation dialogue box.

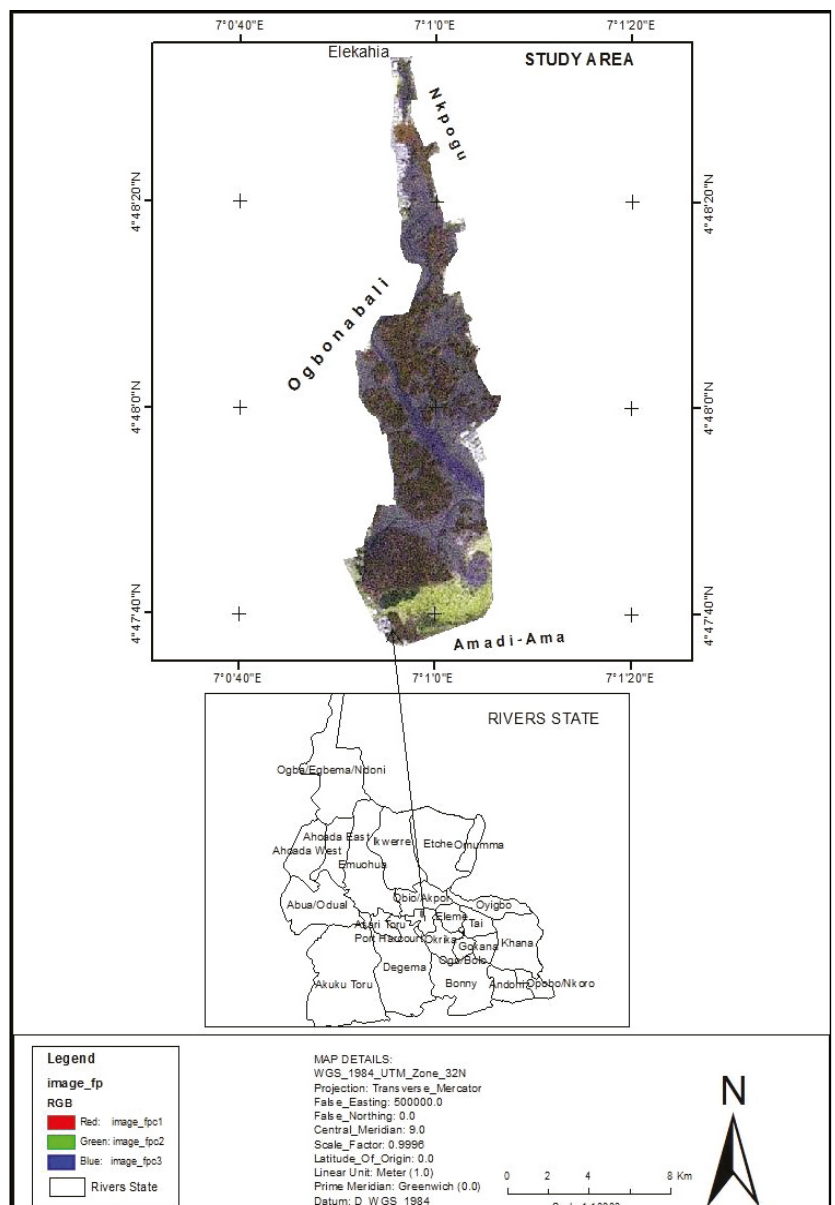


Figure 4: Map of Ogunabali floodplain.

The elevation of the floodplain ranges from -0.32m to 8.1m as obtained from filed survey data. The geology of the floodplain is characterized by sedimentary rocks of the Niger Delta (Youdewei and Nwankwoala, 2016). The mean temperature in Port Harcourt city ranges from 30.0 - 33.0°C and annual rainfall ranges between 2100 – 4600mm (NIMET, 2011). The prevailing rainfall has been responsible for flood cases in the city. This study will proffer solutions on flood management using GIS software and remote sensing approach.

IV. Results and Discussion

This section presented the results of the analysis of floodplain from the observed topographic survey data. The section was sub-divided to address outlined study objectives.

4.1 Modeling Floodplain Elevation

Figure 5 is the spot heights from topographic survey of the floodplain. The data was acquired using total station instrument in coordinate mode. The minimum, maximum and mean elevation were -0.32m, 8.10m, and 1.21m respectively.

Similarly, figure 6 is the contour model of Ogbunabali floodplain. The contour model was produced at contour interval (CI) of 0.10m and the contour line and values represented in brown colour. Contour model is a 2.5D representation of the topography utilized in floodplain modeling.

Triangular Irregular Network (TIN) model is another digital elevation model technique used in floodplain hydrology as shown in figure 7 below. TIN model was produced from the topographic data using the default nine (9) class intervals. The classes are represented using different colours, for example, the maximum elevation with values ranges from 6.831m – 7.724m is shown in Arctic white colour, it is followed by 5.938m – 6.831m as shown in gray colour. The least TIN elevation values range from -0.313m – 0.580m represented by Beryl green colour.

Figure 8 is the slope model of the floodplain produced from the converted TIN model to raster surface. The slope model was produce using the degree of slope and classified into nine (9) default classes. The slope values were presented from the smallest range to the highest range with different colours. The first and the least degree of slope range from 0.00 – 0.47 degrees, followed by 0.47 – 1.10 degrees. The highest slope ranges from 10.33 – 13.31 degrees as shown in red colour.

4.2 Modeling Floodplain Hydrology and Hydraulic Patterns

Figure 9 is the flow accumulation model of the floodplain. Flow accumulation model creates a raster of accumulated

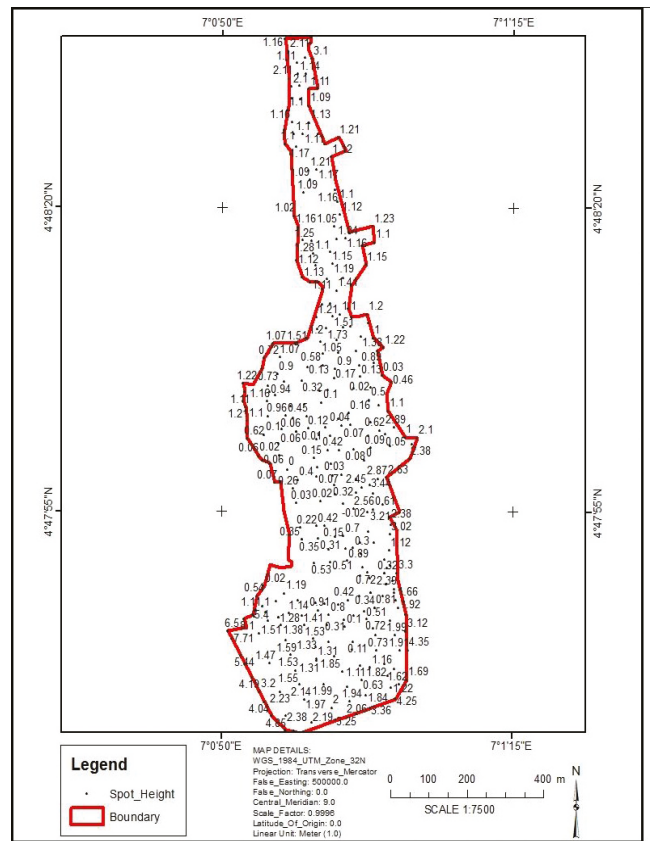


Figure 5: Spot heights of Ogbunabali floodplain.

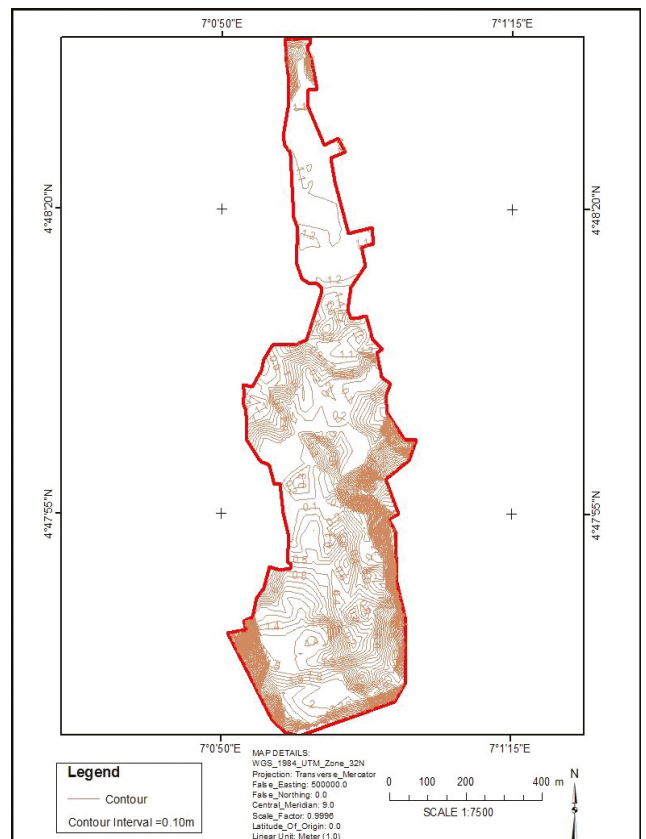


Figure 6: Contour model of Ogbunabali floodplain.

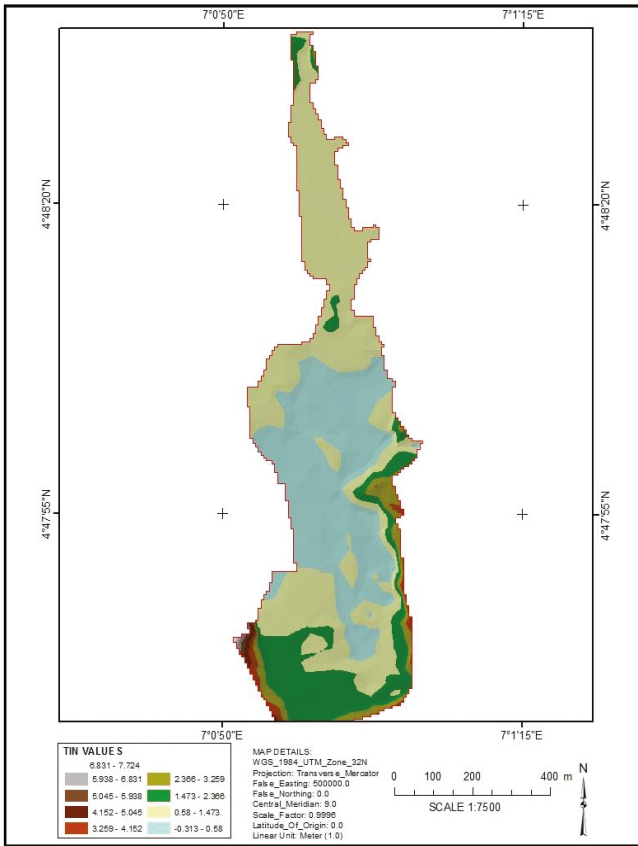


Figure 7: Triangular Irregular Network (TIN) model of Ogunbabi floodplain.

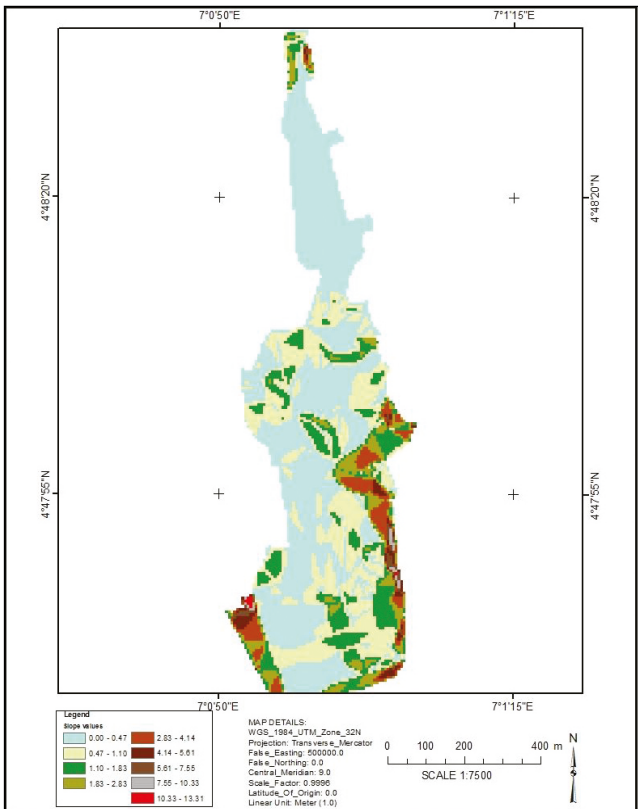


Figure 8: Slope model of Ogunbabi floodplain.

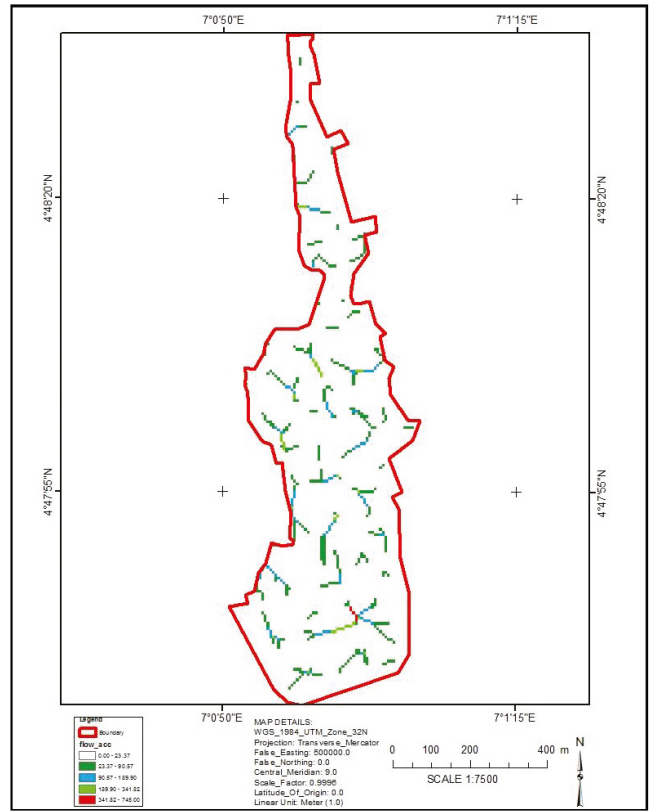


Figure 9: Flow accumulation model of Ogunbabi floodplain.

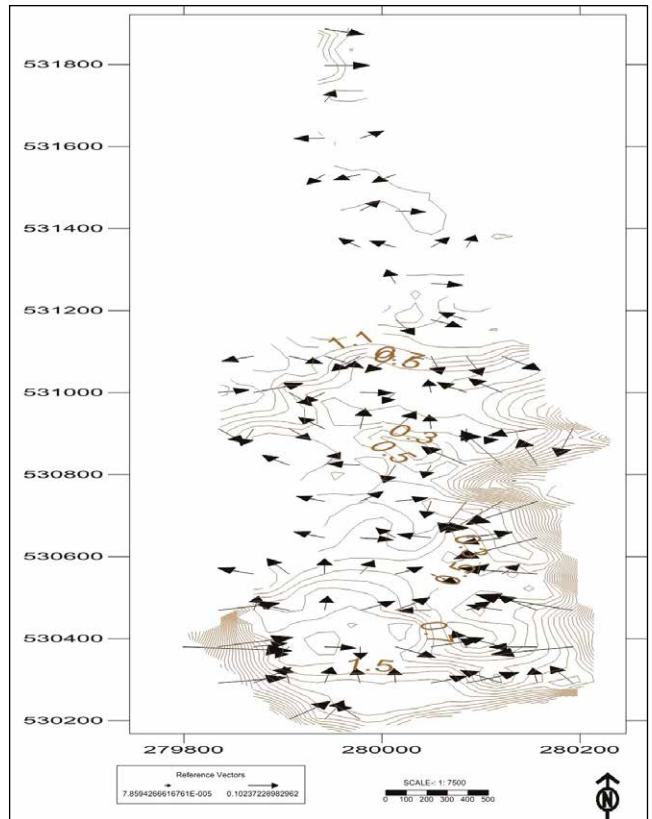


Figure 10: Flow direction model using 1-Grid vector map and overlaid on contour model.

flow into each cell. It was produced from flow direction raster model obtained from digital elevation model (DTM) using hydrology tool in the ArcGIS 10.1 spatial analyst tools. The model was reclassified into five classes from minimum (0.00) to the maximum (745) accumulated flow using natural breaks interval. The minimum accumulated flow cells range from 0.00 – 23.37 represented in white colour followed by 23.37 - 90.57 accumulated flow. The third-class ranges from 90.57 – 189.90 which was followed in the order by 189.90 – 341.82 represented with medium apple green colour. The final class ranges from 341.82 – 745.00 as shown in Mars red colour.

Figure 10 is the flow direction model overlay on contour model of the floodplain. Flow direction model was produced from SURFER 10 using 1-Grid Vector Map command. The model arrows show the direction of water flow in the floodplain. Also, the length of the arrow depends on the magnitude, or steepness of the slope. From the model high flow is represented with longer arrows with magnitude 0.102 while low flow is shown by shorter arrows with magnitude 0.00008 as shown in the model legend.

Table 2: Area of Each Feature Class in the Geodatabase.

Feature Class	Area (ha)
Built-up	4.413
Dumpsite	0.626
Nypa palm	16.583
Water body	21.324

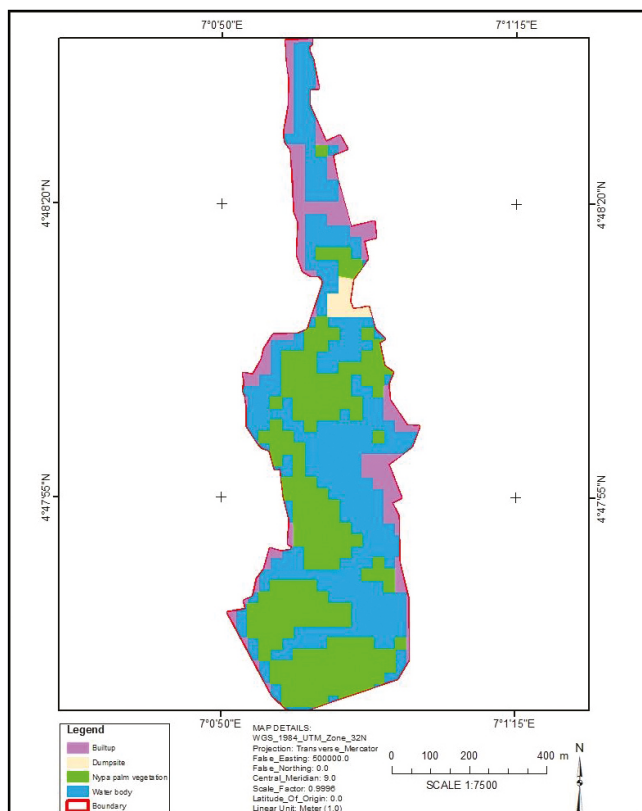


Figure 11: Geodatabase of Ogunabali floodplain.

4.3 Floodplain Digital Database

Floodplain geodatabase was created in ArcGIS 10.1 using SPOT image and the data from field survey and the map is shown in figure 11 below. The floodplain is made up of built-up areas, nypa palm vegetation, water body, and dumpsite in vector polygons. The area in hectares of each feature is shown in table 2 below.

4.4. Discussion of Results

4.4.1 Hydrology and Hydraulic patterns of the Floodplain

The hydraulic modeling of the floodplain shows that the flow patterns are in different direction of the upland area. The contour lines were crowded at three locations namely: extreme north, east and southwest positions, indicating steep slope. However, at the central position of the floodplain, the contour lines are evenly spaced, indicating gentle slope topography. It then implies that water and materials will flow from steep slope to gentle slope. Similarly, TIN model also shows steep slope at the edges with values 3.259m to 8.831m and gentle slope with values -0.313 to 2.366m in the floodplain centre. The maximum slope angle occurs at the edges with value 10.33 – 13.31 degrees as shown in red colour on the slope model. The slope angle at the centre varies from 0.00 – 0.47 and from 0.47 - 1.10 degrees respectively. The hydraulic pattern of the floodplain is further explained using flow direction and accumulation models to represents the actual flow in the area.

The flow direction model shows high flow magnitude on the steep slope represented by long arrows with value 0.102 magnitude. The arrows are pointing towards the floodplain centre with gentle slope (small slope angle). Also, at the floodplain centre the arrows are smaller which indicates that flow magnitude is smaller compared to the edges. The directions of the longer arrows reflect the topography and proved that flood water will flow from steep slope (higher gradient) to gentle slope (lower gradient) area.

The flow accumulation model shows the maximum flow accumulated cell with value ranges from 341.82 – 745.00 in red colour at the southern map area. This high flow accumulation raster cells can be used to channel water from the floodplain. In most cases they defined stream flow in the floodplain and are the resultant of flows from other directions.

4.4.2 Digital Database of the Floodplain

The digital database of the floodplain shows total built-up area as 4.413ha, located at the fringes of the floodplain. The built-up are located along the water course and from the activities of gradual land reclamation. Dumpsite with total area 0.626ha was found within the floodplain while some are being dumped indiscriminately into the water body. The dumpsite is gradually covering the available flow channel as observed at 662m

southward. Similarly, the nypa palm predominantly located in the south with a total area of 16.583ha and is the second largest feature in the floodplain. Such a database will be useful in the management and planning of the floodplain resources and features. It would provide inventories of all features for effective floodplain development. In addition, floodplain database is used to implement the National Floodplain Insurance Program (NFIP) which provides protection of lives and properties for those living in floodplains (West Virginia Quick Guide, 2009). Also, the database will depict flood vulnerable areas, risk zones on Special Flood Hazard Area (SFHA) map. Above all, it will provide relevant information on flood forecasting and early warning to those living in floodplains.

V. Conclusion

The knowledge of floodplain hydrology and hydraulic (H&H) characteristics is essential for the effective management of its resources. The H&H data are incorporated into the floodplain digital database which guaranteed automatic data storage, editing, and retrieval. The study utilized contour model, Triangular Irregular Network (TIN) model, slope model, flow direction and accumulation models derive from topographic survey data of the Ogbunabali floodplain. The hydraulic patterns derive from the models are the same and shows that the flows are from the higher slope along the edges to the lower slope of the floodplain centre.

VI. Recommendations

For further study, the following recommendations were made:

1. That the digital database of all floodplains in Port Harcourt city should be developed for the effective management of flood disaster in the city.
2. That high resolution satellite image should be used to create floodplain database that will aid estimation of flood damage.

3. Establishment of insurance policy for individual living within floodplains areas in the city based on the floodplain base map.

References

- [1] **Association of State Floodplain Managers, (2008)**. Natural and Beneficial Floodplain Functions: Floodplain Management – More than Flood Loss Reduction, 2809 Fish Hatchery Road, Madison, WI 53713, pp. 1-8
- [2] **Anji, M. R. (2008)**. The Textbook of Remote Sensing and Geographic Information Systems, 3rd Edition, 4-4-309, Giriraj Lane, Sultan Bazar, Hyderabad-500 095-A. P, p92.
- [3] **Bera, J., Kartic, B., Moumita, P. (2012)**. Application of RS & GIS in Flood Management A Case of Mongalkote Blocks, Burdwan, West Bengal, India, International Journal of Scientific and Research Publications, Vol. 2, No. 11, pp. 1-9.
- [4] **Charles, D. G., and Paul, R. W. (2008)**. Elementary Surveying an Introduction to Geomatics, 12th Edition, Pearson Education, Inc, Upper Saddle River, New Jersey 07458, pp. 831.
- [5] **Department of Natural Resources, (2006)**. Floodplains and Floodplain Management, DNR Waters in St. Paul 500 Lafayette Road St. Paul, MN 55155-4032, pp. 1-2.
- [6] **Dano, U. L., Abdul-Nasir, M., Ahmad, M. H., Imtiaz, A. C. (2011)**. Geographic Information System and Remote Sensing Applications in Flood Hazards Management: A Review, Research Journal of Applied Sciences, Engineering and Technology, Vol. 3, No. 9, pp. 933-947.
- [7] **Dean, B. G. (2009)**. Analysis of LiDAR Elevation Data for Improved Identification and Delineation of Lands Vulnerable to Sea-Level Rise, Journal of Coastal Research, No. 53, pp. 49-58.
- [8] **DHI (Danish Hydraulic Institute), (2007)**. Mike 21 Flow Model Hydrodynamic Module User's Guide, pp. 1-90.
- [9] **FEMA 480, (2005)**. National Flood Insurance Program (NFIP) Floodplain Management Requirements. A Study Guide and Desk Reference for Local Officials – FEMA480, pp. 8.
- [10] **Heywood, I., Cornelius, S., and Carver, S. (2006)**. An Introduction to Geographic Information System, 3rd Edition, Pearson Education Limited, Edinburgh Gate Harlow Essex CM20 2JE England, pp. 77, 91.
- [11] **Hiremath, P. S., and Kodge, B. G. (2010)**. Generating Contour Lines using Different Elevation Data File Formats, International Journal of Computer Science and Application, Vol. 3, No.1, pp. 19-25.
- [12] **HEC-RAS (Hydrologic Engineering Centre- River Analysis System), (2016)**. User's Manual, Version 5.0, CPD-68, U.S. Army Corps of Engineers, Davis, CA 95616, pp. 1-960.
- [13] **Jay, S. A. (2010)**. Latest LiDAR and Sensor Technologies for Mapping Applications, Northrop Grumman, pp. 1-31.
- [14] **Kavanagh, B. F. (2010)**. Surveying with Construction Applications, 7th Edition, Pearson Education, Inc, Publishing as Prentice Hall, One Lake Street, Upper Saddle River, New Jersey, 07458, pp. 125.
- [15] **Leadership New Paper, (July 29, 2017)**. <http://leadership.ng/2017/07/29/rage-port-harcourt-creeks/>

- [16] **Lawal, D. U., Matori, A. N., Yusuf, K. W., Hashim, A. M., and Balogun, A. L. (2014).**
- [17] Analysis of the Flood Extent Extraction Model and the Natural Flood Influencing Factors: A GIS-based and Remote Sensing Analysis, 8th International Symposium of the Digital Earth (ISDES), IOP Conf. Series: Earth and Environmental Science Vol. 18, pp. 1-6.
- [18] **Lynn, E. J. (2009).** Geographic Information Systems in Water Resources Engineering, 1st edition, CRC Press Taylor & Francis Group Boca Raton London New York, pp. 193.
- [19] **Lee, I-C., Liang, C., and Ron, L. (2010).** Optical Parametric Determination for Mean-Shift Segmentation-Based Shoreline Extraction Using LiDAR Data, Aerial Orthophotos, and Satellite Imagery, ASPRS 2010 Annual Conference San Diego, California, April 26-30, 2010, pp. 1-8.
- [20] **Otto, H., and Rolf, A. (2009).** Principles of Geographic Information Systems, ITC Educational Textbook Series, International Institute for Geo-Information Science and Earth Observation, Enschede, pp. 78.
- [21] **Muhammad, S. P. (2009).** Coastal Changes Assessment Using Multi Spatio-Temporal Data for Coastal Spatial Planning Parangtritis Beach Yogyakarta Indonesia, Master Degree Thesis, Gadjah Mada University, pp. 56.
- [22] **Muhammad, I., and Iyortim, O. S. (2013).** Application of Remote Sensing (RS) and Geographic Information Systems (GIS) in Flood Vulnerability Mapping: Case Study of River Kaduna, International Journal of Geomatics and Geosciences, Vol. 3, No. 3, pp. 618-627.
- [23] **NIMET, (2011).** Nigeria Climate Review Bulletin, pp. 1-40.
- [24] **NOAA, (2012).** Lidar 101: An Introductory to LiDAR Technology, Data, and Applications, National Oceanic and Atmospheric Administration (NOAA) Coastal Services Center, 2234 S. Hobson Ave. Charleston, SC 29405, www.csc.noaa.gov., pp. 1-76.
- [25] **North Carolina Cooperating Technical State, (2003).** LiDAR and Digital Elevation Data, pp. 1-6.
- [26] **Punmia, B. C., Jain, A. K., and Jain, A. K. (2005).** Surveying Vol. 11, Fifteenth Edition, Laxmi Publication (P) Limited, 113 Golden House, Daryaganj, New Delhi – 110002, India, pp. 523.
- [27] **Richards, J. A., and Xiuping, J. (2006).** Remote Sensing Digital Image Analysis, 4th Edition, Springer-Verlag Berlin Heidelberg, Germany, pp.397.
- [28] **Sulebak, J. R. (2000).** Application of Digital Elevation Models, DYNAMAP, White Paper, pp. 1-11.
- [29] **Samarasinghe, S. M. J. S., Nandalal, H. K., Weliwitiya, D. P., Fowze, J. S. M., Hazarika, M.**
- [30] **K., and Samarakoon, L. (2010).** An Application of Remote Sensing and GIS for Flood Risk Analysis: A Case Study at Kalu- Ganga River, Sri Lanka, International Archives of the Photogrammetry, Remote Sensing and Spatial Information Science, Vol. XXXVIII, Part 8, Kyoto Japan 2010, pp. 110-115.
- [31] **Task Force on the Natural and Beneficial Function of the Floodplain, (2002).** The Natural & Beneficial Functions of Floodplains, Reducing Flood Losses by Protecting and Restoring the Floodplain Environment, A Report for the Congress by the Task Force on the Natural and Beneficial Function of the Floodplain, pp. 1-92.
- [32] **Wolman, M. G., and Leopold, L. B. (1957).** River Flood Plains: Some Observations on their Formation, Physiographic and Hydraulic Studies of Rivers Geological Survey Professional Paper 282-C, United States Government Printing Office, Washington, pp. 1-25.
- [33] **Vanguard News Paper, (July 24, 2017).** <https://www.vanguardngr.com/2017/07/photo-flooding-port-Harcourt-heavy-rainfall/>.
- [34] **West Virginia Quick Guide, (2009).** Floodplain Management in West Virginia, West Virginia
- [35] Division of Homeland Security and Emergency, Bldg. 1, Room EB-80, 1900 Kanawha Blvd, East Charleston, pp. 1- 82.
- [36] **www.aerometric.com/ LiDAR.** Light Detection and Ranging Geospatial Solution, LIDSS- 120528.
- [37] **Youdeowei, P. o., and Nwankwoala, H. O. (2016).** Analysis of Soil and Sub-Soil Properties Around Veritas University, Obehie, Southeastern Nigeria, African Journal of Engineering Research, Vol. 4, No. 1, pp. 6-10.
- [38] **Zhilin, L., Qing, Z., and Christopher, G. (2005).** Digital Terrain Modeling Principles and Methodology, CRC Press, 2000 N. W. Corporate Blvd., Boca Raton, Florida 33431, pp. 59, 236.

The paper is originally published in Journal of Research in Environmental and Earth Sciences Volume 9 ~ Issue 12 (2023) pp: 19-35 with open access at www.questjournals.org. © The author(s) 2023.

The paper is republished with authors' permission. ▽

GNSS Constellation Specific Monthly Analysis Summary: November 2024

The analysis performed in this report is solely his work and own opinion. State Program: U.S.A (G); EU (E); China (C) "Only MEO- SECM satellites"; Russia (R); Japan (J); India (I)



Narayan Dhital

Actively involved to support international collaboration in GNSS-related activities. He has regularly supported and contributed to different workshops of the International Committee on GNSS (ICG), and the United Nations Office for Outer Space Affairs (UNOOSA). As a professional employee, the author is working as GNSS expert at the Galileo Control Center, DLR GfR mbH, Germany.

Introduction

The article is a continuation of monthly performance analysis of the GNSS constellation. Please refer to previous issues for past analysis. The new topic for analysis in this issue is the application of 1 Pulse Per Second (1 PPS) signal in Internet of Things (IoT) devices. A simple demonstration with a low cost GNSS module and a microcontroller is provided.

Analyzed Parameters for November, 2024

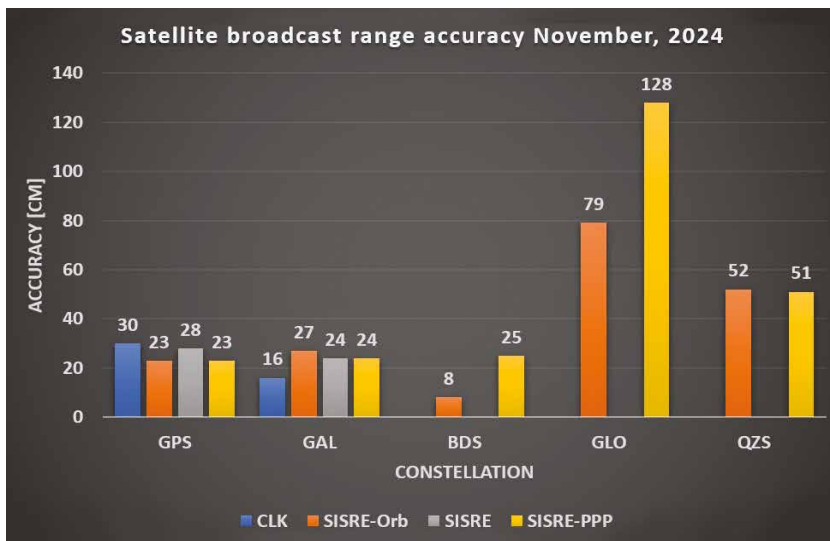
(Dhital et. al, 2024) provides a brief overview of the necessity and applicability of monitoring the satellite clock and orbit parameters.

- a. Satellite Broadcast Accuracy,

measured in terms of **Signal-In-Space Range Error (SISRE)** (Montenbruck et. al, 2010).

- b. **SISRE-Orbit** (only orbit impact on the range error), SISRE (both orbit and clock impact), and **SISRE-PPP** (as seen by the users of carrier phase signals, where the ambiguities absorb the unmodelled biases related to satellite clock and orbit estimations. Satellite specific clock bias is removed) (Hauschlid et.al, 2020)
- c. **Clock Discontinuity**: The jump in the satellite clock offset between two consecutive batches of data uploads from the ground mission segment. It is indicative of the quality of the satellite atomic clock and associated clock model.
- d. **URA**: User Range Accuracy as an indicator of the confidence on the accuracy of satellite ephemeris. It is mostly used in the integrity computation of RAIM.
- e. **GNSS-UTC offset**: It shows stability of the timekeeping of each constellation w.r.t the UTC
- f. **1 PPS**: 1 Pulse Per Second signal is a highly accurate timing reference generated by GNSS receiver, providing a precise pulse every second for synchronization and timekeeping applications.

(a), (b) Satellite Clock and Orbit Accuracy (monthly RMS values)



Note:- for India's IRNSS there are no precise satellite clocks and orbits as they broadcast only 1 frequency which does not

allow the dual frequency combination required in precise clock and orbit estimation; as such, only URA and Clock Discontinuity is analyzed.

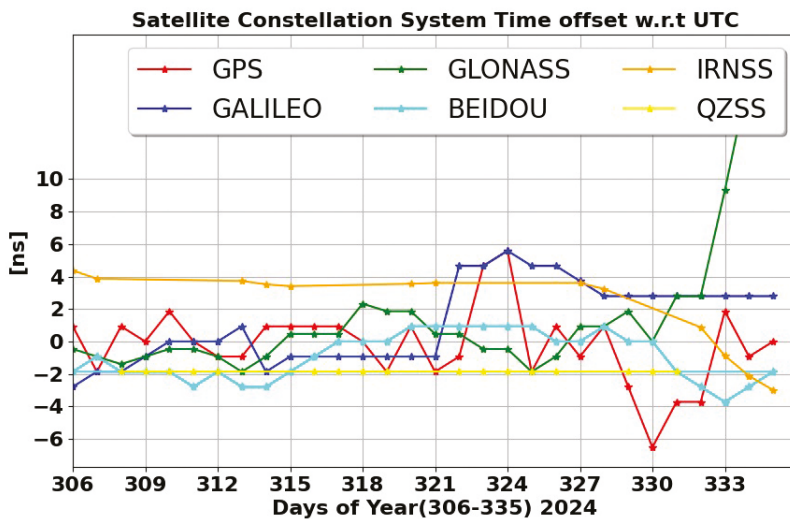
(c)-1 Satellite Clock Jump per Mission Segment Upload

Const	Mean [ns]	Max [ns]	95_Percentile [ns]	99_Percentile [ns]	Remark (Best and Worst 95 %)
IRNSS	4.48	544.02	7.31	32.74	Best I02 (4.48 ns) Worst I06 (16.77 ns) Big jumps for each satellite in multiple days
GPS	11.63	145425.84	1.05	2.36	Best G15 (0.39 ns) Worst G26 (2.72 ns) Very large jumps for G26 on multiple days, relatively large jump for G19, G17, G06, G02, G03, G05 on different occasions
GAL	0.08	3.44	0.17	0.39	Best E03 (0.14 ns) Worst E19 (0.34 ns). E11 had a few low amplitude jumps.

(d) User Range Accuracy (Number of Occurrences in Broadcast Data 01-30 November)

IRNSS-SAT	2 [m]	2.8 [m]	4.0 [m]	5.7 [m]	8 [m]	8192 [m]	9999.9 [m]	Remark Other URA values (frequency)
I02	2899	14	2	-	1	-	-	-
I03	-	-	-	-	-	-	-	-
I06	640	42	4	-	-	-	-	-
I09	524	2	1	-	2	-	-	-
I10	445	1	-	-	1	1	-	-

(e) GNSS-UTC Offset



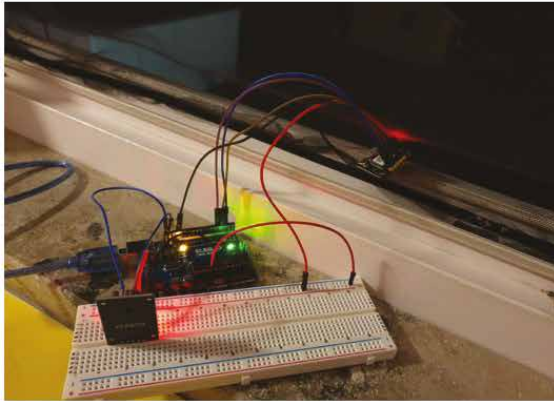
(f) GNSS 1 PPS Signal for IoT Devices

IoT devices are ubiquitous in the modern world, enabled by the miniaturization and low cost of sensors, which allow interconnected devices and services to operate seamlessly. A crucial component in this ecosystem is the 1 PPS signal. The combination of the 1 PPS signal and GPS UTC time provides precise time tagging for various sensors and serves as a synchronization medium for a network of sensors. Most devices incorporate an internal oscillator (crystal or TCXO) for timekeeping, offering reasonable accuracy, typically within a minute per year. However, multiple time sources, including LTE cell

networks, NTP, and GNSS time, are often utilized. One commonly used RTC in sensors and devices is the DS3231, which features an integrated crystal oscillator and temperature compensation, making it less susceptible to temperature variations.

Using the GT U7 GPS module with an Arduino UNO R3 microcontroller for GNSS time applications involves leveraging the 1 PPS signal for precise time tagging and synchronization of sensors in IoT devices. The 1 PPS signal provides a highly accurate timing reference, which can be used to synchronize the internal clocks of various sensors, ensuring consistent data collection. By connecting the 1 PPS output of the GT U7 GPS module to an interrupt pin on the Arduino, the time between pulses can be measured to maintain synchronization. This method is particularly useful in the absence of Network Time Protocol (NTP) servers, as the GPS 1 PPS signal serves as a reliable time source, often used in NTP stratum 1 servers.

In this demonstration, the setup is illustrated in Figure f(a). The RTC and GT U7 GPS module are both connected to the microcontroller through data pins, with the Arduino IDE used for control and code execution. The bottom left of Figure f(a) shows the steering of the RTC using the GPS 1 PPS signal. Initially, the RTC was set to a random time, and after a few seconds, steering was initiated via a control command. The RTC time was immediately synchronized to the GPS-derived CET time. Due to processing delays and resource overload on the microcontroller, the printed output (for demonstration purposes) of the RTC time and the CET time shown on the internet may not match, but they are synchronized in principle. After a few minutes, the steering was stopped, and the RTC was left to run freely. After 10 days, the RTC time was compared against the UTC time, as shown in the top right of Figure f(a). The RTC time had advanced by more than 2 seconds, consistent with the reported accuracy of 2 ppm for DS3231 oscillator (approximately 1 minute per year).



local	2024-12-08 19:33:28	Sunday	day 343	timezone UTC+1
UTC	2024-12-08 18:33:28	Sunday	day 343	MJD 60652 77324
GPS	2024-12-08 18:33:46	week 2344	66826 s	cycle 2 week 0296 day 0
Loran	2024-12-08 18:33:55	GRI 9940	215 s until	next TOC 18:37:03 UTC
TAI	2024-12-08 18:34:05	Sunday	day 343	10 + 27 leap seconds = 37

```

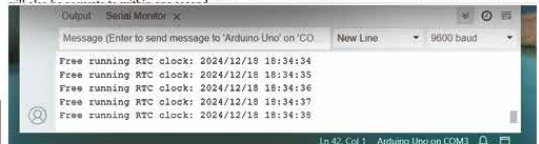
RTC Time: 2024/12/8 19:33:26
1PPS Steered RTC Time (CET/CEST): 2024/12/8 19:33:26
1PPS detected. GPGGA:
RTC Time: 2024/12/8 19:33:27
1PPS Steered RTC Time (CET/CEST): 2024/12/8 19:33:27
  
```



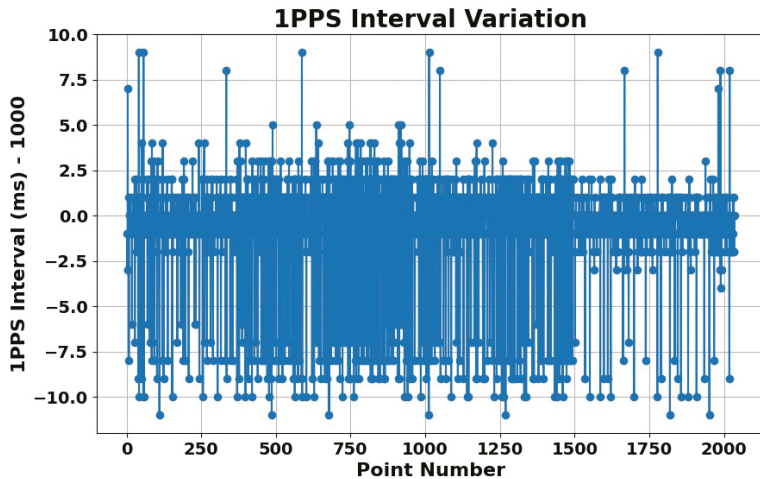
d on your PC clock:

local	2024-12-18 19:34:35	Wednesday	day 353	timezone UTC+1
UTC	2024-12-18 18:34:35	Wednesday	day 353	MJD 60662 77401
GPS	2024-12-18 18:34:53	week 2345	326093 s	cycle 2 week 0297 day 3
Loran	2024-12-18 18:35:02	GRI 9940	431 s until	next TOC 18:41:46 UTC
TAI	2024-12-18 18:35:12	Wednesday	day 353	10 + 27 leap seconds = 37

date/time reported by your PC (as seen by your web browser). If your PC clock is accurate to a second then it



f (a): The demonstration setup of a low-cost GPS module 1 PPS signal for IoT devices. Top left part shows the connection of the GT U7 GPS module connected to the antenna (in the window, very moderate satellite visibility) and controlled by the microcontroller unit. The Real Time Clock module is also connected to the MCU. While bottom left shows the 1 PPS steered RTC time (CET), top right shows the free running time (UTC) of the RTC.



f (b): The jitter in the GPS 1 PPS signal interrupted by the service routine of the used microcontroller.

Regarding the 1 PPS signal, the Arduino interrupt service routine reported slight variations in the 1 PPS timing (e.g., 1000 ms, 999 ms, 1001 ms) of the rising edge from the digital pin. These discrepancies can be attributed to factors such as inherent jitter in the GPS signal and processing delays within the Arduino. A jitter of 1 to 10 ms, as shown in Figure f(b), is relatively high and not typical for most GPS

modules, where jitter is usually in the range of nanoseconds to microseconds. Additionally, GPS satellite visibility and signal obstruction can affect the stability of the 1 PPS signal. The setup in Figure f(a) indicates poor signal quality in the surrounding environment. Furthermore, the microcontroller may introduce additional delays due to its processing limitations. The goal of this demonstration is to showcase the

synchronization of the RTC module with the 1 PPS signal, ensuring that the RTC maintains reliable time for the majority of IoT sensors, even when the GPS signal is unavailable or degraded.

Note: as the above demonstration is only meant for an information purpose on the application of GNSS timing on IoT sensors, no references are mentioned. The used hardware was randomly selected based on the availability. There are plenty of materials on the internet related to 1 PPS based timing for such applications.

Monthly Performance Remarks:

- Satellite Clock and Orbit Accuracy:
 - Except Beidou and Galileo, degradation in performances is noticed for other constellation.
 - For GPS, the clock performances look degraded for multiple satellites on different days.
 - For QZSS, the performance of orbits is highly degraded for the time 318-323 day of year.
 - For IRNSS, URA value distribution for all satellites shows low spread than before.

2. UTC Prediction (GNSS-UTC):
- All constellations show stable UTC prediction with minor variations. GPS and Galileo both provided slightly diverging values on couple of occasions. GLONASS started to diverge at the end of the month.

References

Alonso M, Sanz J, Juan J, Garcia, A, Casado G (2020) Galileo Broadcast Ephemeris and Clock Errors Analysis: 1 January 2017 to 31 July 2020, MDPI

Alonso M (2022) Galileo Broadcast Ephemeris and Clock Errors, and Observed Fault Probabilities for ARAIM, Ph.D Thesis, UPC

BIMP (2024 a) https://e-learning.bipm.org/pluginfile.php/6722/mod_label/intro/User_manual_cggts_analyser.pdf?time=1709905608656

BIMP (2024 b) <https://e-learning.bipm.org/mod/folder/view.php?id=1156&forceview=1>

BIMP (2024 c) <https://cggts-analyser.streamlit.app>

Cao X, Zhang S, Kuang K, Liu T (2018) The impact of eclipsing GNSS satellites on the precise point positioning, Remote Sensing 10(1):94

Dhital N (2024) GNSS constellation specific monthly analysis summary, Coordinates, Vol XX, Issue 1, 2, 3, 4

Hauschlid A, Montenbruck O (2020) Precise real-time navigation of LEO satellites using GNSS broadcast ephemerides, ION

Guo F, Zhang X, Wang J (2015) Timing group delay and differential code bias corrections for BeiDou positioning, J Geod,

IERS C04 (2024) <https://hpiers.obspm.fr/iers/eop/eopc04/eopc04.1962-now>

IGS (2021) RINEX Version 4.00 https://files.igs.org/pub/data/format/rinex_4.00.pdf

Li M, Wang Y, Li W (2023) performance evaluation of real-time orbit determination for LUTAN-01B satellite using broadcast earth orientation parameters and multi-GNSS combination, GPS Solutions, Vol 28, article number 52

Li W, Chen G (2023) Evaluation of GPS and BDS-3 broadcast earth rotation parameters: a contribution to the ephemeris rotation error

Liu T, Chen H, Jiang Weiping (2022) Assessing the exchanging satellite attitude quaternions from CNES/CLS and their application in the deep eclipse season, GPS Solutions 26(1)

Montenbruck O, Steigenberger P, Hauschlid A (2014) Broadcast versus precise ephemerides: a multi-GNSS perspective, GPS Solutions

Montenbruck O, Hauschlid A (2014 a) Differential Code Bias Estimation using Multi-GNSS Observations and Global Ionosphere Maps, ION

Steigenberger P, Montenbruck O, Bradke M, Ramatschi M (2022) Evaluation of earth rotation parameters from modernized GNSS navigation messages, GPS Solutions 26(2)

Sylvain L, Banville S, Geng J, Strasser S (2021) Exchanging satellite attitude quaternions for improved

GNSS data processing consistency, Vol 68, Issue 6, pages 2441-2452

Walter T, Blanch J, Gunning K (2019) Standards for ARAIM ISM Data Analysis, ION

Wang N, Li Z, Montenbruck O, Tang C (2019) Quality assessment of GPS, Galileo and BeiDou-2/3 satellite broadcast group delays, Advances in Space Research

Wang J, Huang S, Lia C (2014) Time and Frequency Transfer System Using GNSS Receiver, Asia-Pacific Radio Science, Vol 49, Issue 12


<https://cggts-analyser.streamlit.app>

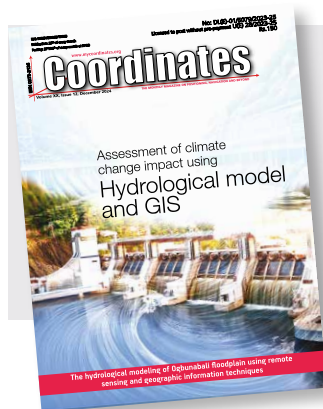
Note: References in this list might also include references provided to previous issues.

Data sources and Tools:

<https://cddis.nasa.gov> (Daily BRDC); http://ftp.aiub.unibe.ch/CODE_MGEX/CODE/ (Precise Products); BKG “SSRC00BKG” stream; IERS C04 ERP files

(The monitoring is based on following signals- GPS: LNAV, GAL: FNAV, BDS: CNAV-1, QZSS:LNAV IRNSS:LNAV GLO:LNAV (FDMA))

Time Transfer Through GNSS Pseudorange Measurements: <https://e-learning.bipm.org/login/index.php> Allan Tools, https://pypi.org/project/AllanTools/gLAB_GNSS, <https://gage.upc.edu/en/learning-materials/software-tools/glab-tool-suite> 



Download your copy from
www.mycoordinates.org

YellowScan teams up with Argosdyne

YellowScan has announced a collaboration with Argosdyne, whose latest UAV has officially received the C2 Class certification. The C2 Class certification permits closer operation to bystanders and in densely populated areas, meeting stringent European safety requirements. www.yellowscan.com

ESA and Japan expand collaboration in space exploration

The European Space Agency (ESA) and the Japan Aerospace Exploration Agency (JAXA) have signed a new joint statement to deepen their partnership across asteroid, lunar, and planetary exploration. Signed on November 20 by ESA Director General Josef Aschbacher and JAXA President Yamakawa Hiroshi in Tsukuba, Ibaraki, the agreement builds on decades of successful collaboration.

The two agencies share a history of joint missions, including BepiColombo's journey to Mercury and EarthCARE's study of Earth's climate. ESA and JAXA astronauts have also worked together aboard the International Space Station, forging a strong foundation for future endeavors. Under the latest agreement, ESA and JAXA will accelerate collaborative studies for the Ramses mission to the asteroid Apophis, which will pass Earth in 2029. Potential contributions from JAXA include thermal infrared imaging, solar array technology, and launch services.

The partnership extends to lunar exploration, where the two agencies are working within the framework of the Artemis program. ESA's Argonaut lunar cargo lander and JAXA's pressurized lunar rover are central components of this effort. Additionally, ESA's recently inaugurated lunar analogue facility may serve as a testing ground for JAXA's lunar technologies. Collaborative efforts could also involve small commercially provided lunar rovers, the lunar polar exploration mission, and the Moonlight program to establish a lunar communications and navigation satellite network.

ESA and JAXA are also advancing discussions on Mars exploration, aiming to leverage technologies such as electric propulsion and descent systems to send small landers to the Red Planet. www.spacedaily.com

China tested its first inflatable space module in orbit

China tested out a small expandable module in orbit during the recent Shijian-19 mission, an update more than a month after the spacecraft's landing reveals. The China Academy of Space Technology (CAST), which manufactured both Shijian-19 and the test module, revealed that the "inflatable flexible sealed module" completed an on-orbit test in a Nov.

The module is described by CAST as a multifunctional sealed structure made from flexible composite materials. The mission was deemed a complete success by CAST, a key division of China's state-owned contractor CASC, which also developed modules for the Tiangong space station. spacenews.com

Joint venture by Space42 and ICEYE

Space42, UAE and ICEYE recently announced the creation of a joint venture to manufacture SAR satellites in the UAE, building on their successful cooperation, which includes the recent launch of the UAE's first SAR satellite, Foresight-1, in August 2024.

This joint venture will directly advance the UAE's Earth Observation (EO) Program, which was created to build national satellite remote sensing and EO capabilities. space42.ai

ESA awards development contract for NanoMagSat

The ESA awarded a contract to Open Cosmos to design, build, launch and commission the NanoMagSat Scout satellites. This new mission will uphold Europe's leadership in

monitoring Earth's magnetic field and contribute to applications such as space weather hazard assessment, navigation, directional drilling, and more.

The Scouts are small satellites that deliver value-added science, either by miniaturising existing space technologies or by demonstrating innovative observing techniques. Notably, the Scout missions embody the principles of New Space, leveraging an agile and cost-effective development process to achieve their goals efficiently. www.esa.int

ISRO & ASA sign Implementing Arrangement for Gaganyaan

An Implementation Agreement (IA) was signed between Indian Space Research Organisation (ISRO) and Australian Space Agency (ASA) on November 20, 2024 for further strengthening cooperation in space activities between Australia and India. The IA enables cooperation between both space agencies on crew and crew module recovery for Gaganyaan missions. The IA was signed by Shri DK Singh, Director, HSFC on ISRO side at Bengaluru and Shri Jarrod Powell, General Manager, Space Capability Branch, on ASA side at Canberra.

ISRO has embarked on the Human Spaceflight ("Gaganyaan") programme with an objective of demonstrating human space flight capability to Low Earth Orbit in an Indian Crew Module with up to three crew members for up to three days and safely recovering them after the mission. The IA enables the Australian authorities to work with Indian authorities to ensure support for search and rescue of crew and recovery of crew module as part of contingency planning for ascent phase aborts near Australian waters.

India and Australia are enduring strategic partners and both space agencies are working closely and are committed to explore current and future collaboration activities. The signing of the IA is another step forward in the cooperation between Indian and Australian space agencies. www.isro.gov.in

Skykraft forms international partnership

Skykraft has announced the formal signing of Participating Project Partner Agreement for the “Demonstration of Collaborative Position Navigation and Timing (PNT) in Low Earth Orbit (LEO)” project. Supported by an International Space Investment (ISI) India Projects grant from the Australian Government, this initiative marks a key step in supporting the growth of joint space projects between Australia and India. ISI India Projects broadly aligns with the India Economic Strategy to 2035, especially regarding the India-Australia Comprehensive Strategic Partnership and the Comprehensive Economic Cooperation Agreement – focusing on strengthening its bilateral relationships and activities with mutual understanding of common interests and shared values, in support of both countries’ prosperity.

The primary goal of the project is the development of next-generation collaborative PNT systems. PNT systems play a critical role in sectors such as transportation, communication, and infrastructure, however existing systems can be prone to errors. For example, the aviation industry has been particularly affected in a growing number of regions, with aircraft navigation systems being impacted or incorrect information being reported to Air Traffic Management (ATM) controllers.

The project will demonstrate the feasibility of large-scale constellations in LEO, address the vulnerability of existing Global Navigation Satellite Systems (GNSS) in denied environments, investigate additional applications for PNT signals that can be exploited from LEO and, through the demonstration of the resilience of large-scale constellations (which can be easily updated and reconstituted), provide a roadmap to enable collaborative LEO-PNT. www.skykraft.com.au

Court greenlights Ligado Networks’ \$39 billion lawsuit

The U.S. Court of Federal Claims has allowed Ligado Networks to move forward with its \$39 billion lawsuit against the federal government, marking a significant

step in a long-running dispute over 5G spectrum usage and property rights.

The dispute stems from the FCC’s 2020 decision granting Ligado exclusive control over spectrum near GPS frequencies, raising concerns about potential interference with GPS systems. In its October 2023 lawsuit, Ligado accused the U.S. government of a “multiyear misinformation and disparagement campaign” to hide its actions and misappropriate Ligado’s licensed spectrum for DOD systems without permission or compensation.

The government sought to dismiss the lawsuit in January 2024, citing lack of jurisdiction and Ligado’s inability to prove a valid property interest in its FCC license. The core of the conflict lies in the proximity of Ligado’s L-band spectrum to GPS frequencies, which could interfere with critical GPS signals used for navigation, timing, and national security. The DOD, GPS companies, and industry officials have strongly opposed Ligado’s plan for a terrestrial 5G network, warning of harmful interference to GPS receivers.

JAVAD GNSS congratulates the GSP on groundbreaking success

JAVAD GNSS proudly extends its congratulations to the Gruyère Space Program (GSP) for their remarkable achievement in developing Colibri, the world’s first student-built reusable rocket hopper. With over 50 successful flights, including an ascent to 105 meters and a precise landing, Colibri represents a historic milestone in student-led aerospace innovation.

A critical component of this success was the TR-2S OEM GNSS receiver, engineered and manufactured by JAVAD GNSS. The receiver provided precise real-time positioning capabilities and maintained a 1cm fix throughout flight, enabling Colibri to achieve its ambitious goals. GSP’s successful deployment of the TR-2S highlights its robustness and performance under demanding conditions. Javad.com

DoD announces strategy for countering unmanned systems

On December 2 US Secretary of Defense Lloyd J. Austin III signed a classified Strategy for Countering Unmanned Systems. The strategy unifies the Department’s approach to countering these systems that looks across domains, characteristics, and timeframes.

Unmanned systems pose both an urgent and enduring threat to U.S. personnel, facilities, and assets overseas. Unmanned aerial systems, most commonly known as drones, pose the most significant threat at this time and increasingly in the US homeland. These threats are changing how wars are fought. By producing a singular Strategy for Countering Unmanned Systems, the Secretary and the Department are orienting around a common understanding of the challenge and a shared approach to addressing it. www.defense.gov

Propeller Drones wins contract

Propeller Drones has secured a \$7 million contract with the Israel Electric Corporation (IEC) to conduct fully autonomous UAV operations for electrical infrastructure inspection. This project marks an advancement in beyond visual line of sight (BVLOS) drone operations in Israel, as it represents the first government approval for pre-approved BVLOS flights using an unmanned traffic management (UTM) system.

Under the collaboration, Propeller Drones and FlightOps will partner to enhance AI flight capabilities that meet IEC requirements and regulatory standards. Airwayz, a company specializing in low-altitude UTM solutions, has been selected to provide the UTM system for managing drone operations. businessnewsthisweek.com

Indian Railways floats Rs 3,200-crore tender for LiDAR system to enhance track safety

The Indian Railways has issued tenders of Rs 3,200 crore for installation of Light Detecting and Ranging (LiDAR) technology on trains and rail tracks.

The LiDAR technology will help detect fractures, faults, and missing sections on the tracks. It will also help the railway develop 3D models of tracks using images from sensors. The technology uses laser beams to map the tracks, identify obstacles, and measure distances. The sensors will be placed on moving trains and at fixed locations along the network to provide real-time data on track conditions. This data can help detect flaws quickly and send alerts to railway officials to prevent derailments and collisions.

The LiDAR system will not only identify track defects but will also help prevent derailments and collisions by providing real-time data. This data can also be analysed to create predictive models that can forecast potential issues before they occur, improving the overall safety. www.moneycontrol.com

NovAtel launches GAJT-310

NovAtel has announced its lowest SWaP (size, weight and power) GNSS Anti-Jam Technology (GAJT) with the launch of the GAJT-310. It is a battle-proven solution for assured positioning, navigation and timing (A-PNT) that protects against hostile radio frequency interference on land, at sea and in the air. It provides users with the latest powerful anti-jam technology with low latency in a smaller device. Low latency means the GAJT-310 can be put to work protecting signals immediately —no additional setup— just plug in and protect. novatel.com

Raytheon awarded contract extension for Space Force GPS OCX program

The U.S. Space Force's Space Systems Command (SSC) has awarded Raytheon a \$196.7 million contract extension for

the GPS Next Generation Operational Control System (OCX) program, despite being several years behind schedule. This new award brings the total value of the OCX contract to nearly \$4.5 billion since its launch in 2010, though the U.S. Government Accountability Office (GAO) estimates the total cost will approach \$8 billion. The OCX program, aimed at upgrading GPS infrastructure, has encountered significant delays, currently running about seven years behind its original timeline. The GAO has reported that the 17-ground station system will not meet its October 2024 deadline, with further testing needed for operational readiness by December 2025.

Despite these setbacks, OCX remains crucial for modernizing GPS capabilities. It will enable full M-Code features, offering jamming-resistant GPS signals for military operations in contested environments, and will enhance cybersecurity for both military and civilian use. Once fully operational, OCX will manage all modernized and legacy GPS satellites, controlling both civil and military navigation signals.

Swift Navigation and CHC Navigation partnership

Swift Navigation has announced its collaboration with CHC Navigation. The partnership integrates Swift's Skylark® Precise Positioning Service with CHC Navigation's high-performance GNSS receivers, delivering reliable and cost-effective centimeter-accurate positioning to unlock the next generation of location-based products such as autonomous vehicles, robotics, and surveying equipment. swiftnav.com

AEVEX Aerospace acquires Veth Research Associates

AEVEX Aerospace has announced the acquisition of Veth Research Associates (VRA). This acquisition strengthens AEVEX's position in providing innovative solutions for operating their unmanned systems in jammed and contested environments. Key to this

acquisition is VRA's LYNX vision-based navigation (VBN) system, which allows for navigation independent of external GPS signals. The LYNX VBN system is day/night capable, modular, and open in design, making it adaptable for use on both manned and unmanned platforms. aevex.com

VIavi expands market reach with Inertial Labs acquisition

Viavi Solutions Inc. (VIavi) has signed a definitive agreement to acquire Inertial Labs, Inc. for initial consideration of \$150 million at closing and up to \$175 million of contingent consideration over four years. The acquisition is expected to add approximately \$50 million to VIavi's Network and Service Enablement (NSE) annual revenue in calendar year 2025. www.viavisolutions.com

ANELLO Photonics raises Series B funding

ANELLO Photonics has announced the successful closure of its Series B funding round. The investment was co-led by Lockheed Martin, Catapult Ventures and One Madison Group. Additional investors included New Legacy, Build Collective, Trousdale Ventures, In-Q-Tel (IQT), K2 Access Fund, Purdue Strategic Ventures, Santuri Ventures, Handshake Ventures, Irongate Capital and Mana Ventures. This funding round will accelerate ANELLO's mission to revolutionize navigation and positioning in GPS-denied environments across both Industrial and Defense applications. www.anellophotonics.com

SparkFun Electronics launches GNSS RTK module for positioning accuracy

SparkFun Electronics has introduced the SparkFun Quadband GNSS RTK Breakout (Qwiic), which is designed to improve positioning accuracy using the Quectel GNSS module. This module has a compact design and compatibility with the Qwiic connector, making it easy to integrate into various projects. Additionally, it shares the same dimensions, pin layout and connectors as

the SparkFun GPS-RTK-SMA Breakout – ZED-F9P, offering a seamless upgrade path for users. www.sparkfun.com

The GEODNET Foundation introduces GEO-PULSE

The GEODNET Foundation is revolutionizing car navigation with the launch of GEO-PULSE - GPS device designed to deliver unprecedented positioning accuracy. Leveraging GEODNET RTK network, GEO-PULSE combines cutting-edge sensor fusion technology with an accessible price point, ensuring every driver can enjoy precision navigation. geodnet.com

New automotive positioning standard for the future of vehicle safety in China

Spirent Communications plc has announced the role of its positioning, navigation and timing (PNT) simulation systems in the creation of a new automotive positioning standard in China. The newly announced GB/T 45086.1-2024 standard sets out the recommended technical and test requirements for on-board vehicle positioning systems such as GNSS and is expected to be adopted as part of China's Accident and Emergency Calling Systems (AECS) framework.

It is expected to underpin the forthcoming AECS framework, which will become a regulatory requirement for all vehicles being sold in China from next year. As China's equivalent to the European eCall, AECS will ensure rapid response in car accidents, potentially saving many lives. By establishing rigorous benchmarks for positioning systems, the new standard aims to enhance the reliability and performance of these critical positioning components. It also has the potential to provide the groundwork for regulation of autonomous vehicles on public roads. www.spirent.com

Leica Geosystems presents new utility detection solution

Leica Geosystems has announced its latest utility detection solution, the Leica

DT100 Precision Locator and Leica DE100 Transmitter. The precision locator market is driven by the need for effective, reliable solutions that enhance safety, efficiency and productivity in various operational contexts. DT100, paired with the DE100 transmitter, offers a robust solution designed to meet the demanding needs of industries like construction, utilities, and telecommunications. <https://leica-geosystems.com>

RIEGL LiDAR technology for BIM and AEC applications

For the first time, RIEGL will be presenting its ultimate surveying solution for the construction sector – the RIEGL VZ-600i 3D terrestrial laser scanner – at BAU 2025, Munich, Germany in January 2025. The RIEGL team will present the numerous advantages of using RIEGL Ultimate LiDARTM Technology in building construction and civil engineering, particularly its integration into the digital BIM process. Practical examples from various BIM phases, such as recording existing structures, quality assurance during construction documentation, will demonstrate the impressive performance of RIEGL technologies. newsroom.riegl.international

u-blox launches new GNSS chip for wearable applications

u-blox launches new GNSS chip for wearable applications featuring ultra-low power consumption and high positioning accuracy in the smallest form factor. The UBX-M10150-CC GNSS is poised to revolutionize the design of compact wearable devices like sports and smart watches. It features pioneering LEAP (Low Energy Accurate Positioning) technology that achieves a mere 10mW power consumption. www.u-blox.com

UAVOS releases next-generation ground control station

UAVOS' new PGCS.7 has a new generation powerful Getac X600 PC, an external redundant power supply, and an improved customizable I/O hardware

interface. Featuring fully redesigned switch buttons, I/O panels allow users to customize to their exact design needs fully. It enables intuitive and user-friendly control making it possible to reduce the likelihood of operator error during missions. Compatible with preferred autopilots, it features flight and mission operation software, video-tracker software, payload sensor data, and information. www.uavos.com

GMV to develop Galileo's emergency aid satellite services

The European Union Agency for the Space Programme (EUSPA) has awarded GMV a FWC contract to deliver new Galileo functionalities under EmeRgency Alerting System (ERAS), allowing EUSPA to provide new Emergency-related services, namely the Emergency Warning Satellite System (EWSS), SAR/Remote Beacon Activation and SAR/Two-Way Communications Emergency. The four-year contract, worth around 6 million euros, will enable significant progress in Europe's response capabilities to natural and man-made disasters. The GMV-led industrial organization includes Ineco, ALTEN Spain, and Kineton as subcontractors.

The new ERAS system will in the first place, allow Member States National Civil Protection Authorities for ondemand broadcast of Emergency Warning messages to be sent directly to the population in areas at risk or already affected by a natural or provoked disaster, which will be transmitted directly by the Galileo satellites to smartphones or any other device capable of receiving signals from these satellites. The system is expected to be fully operational in the first half of 2026. www.gmv.com

Sodex Innovations launches terrain mapping systems

Sodex Innovations has unveiled the SDX-4D Vision and SDX-Compact machine-mounted terrain mapping systems. It integrates advanced sensor technology and artificial intelligence (AI) driven


SUBSCRIPTION FORM

YES! I want my **Coordinates**

I would like to subscribe for (tick one)

1 year 2 years 3 years

12 issues 24 issues 36 issues
Rs.1800/US\$140 Rs.3400/US\$200 Rs.4900/US\$300

* 

First name

Last name

Designation

Organization

Address

.....

City Pincode

State Country

Phone

Fax

Email

I enclose cheque no.

drawn on

date towards subscription

charges for Coordinates magazine

in favour of 'Coordinates Media Pvt. Ltd.'

Sign Date

Mail this form with payment to:

Coordinates
A 002, Mansara Apartments
C 9, Vasundhara Enclave
Delhi 110 096, India.

If you'd like an invoice before sending your payment, you may either send us this completed subscription form or send us a request for an invoice at iwant@mycoordinates.org

* Postage and handling charges extra.

MARK YOUR CALENDAR

February 2025

DGI (Defence Geospatial Intelligence)
10 - 12 February, 2025
London, UK
<https://dgi.wbresearch.com>

Geo Week 2025
10 - 12 February
Denver, USA
www.geo-week.com

MENA Geospatial Forum
24 - 25 February 2025
Dubai, UAE
<https://menageospatialforum.com>

March 2025

Munich Satellite Navigation Summit
26 - 28 March 2025
Munich, Germany
www.munich-satellite-navigation-summit.org

April 2025

Geo Connect Asia
09 - 10 April 2025
Singapore
www.geoconnectasia.com

GISTAM 2025
1-3 April
Porto, Portugal
<https://gistam.scitevents.org>

May 2025

17th Baška GNSS Conference
11-15 May 2025
Baška, Croatia
<https://rin.org.uk>

Geognite
12-14 May 2025
Ottawa, Canada
<https://geognite.ca>

June 2025

GEO Business 2025
04-05 June
London, UK
www.geobusinessshow.com

July 2025

Esri User Conference
14-18 July 2025
San Diego, USA
www.esri.com

September 2025

Commercial UAV Expo 2025
2-4, September
Las Vegas
www.expouav.com

ION GNSS+
08-12 September 2025
Baltimore, USA
www.ion.org

October 2025

Intergeo 2025
7-9 October
Frankfurt, Germany
www.intergeo.de/en

data processing to create digital twins of worksites while the machine operates. Data is uploaded to the SDX Cloud, allowing for real-time analysis from any location. www.sodex-innovations.com

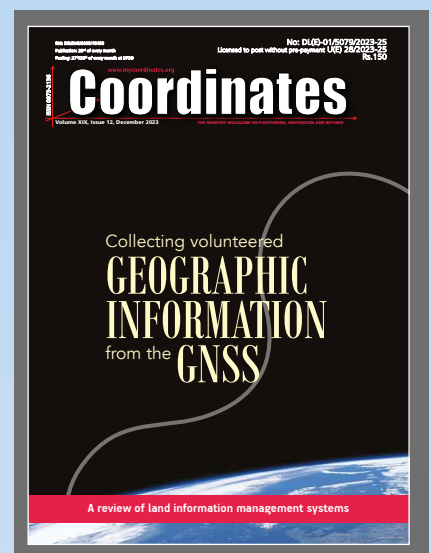
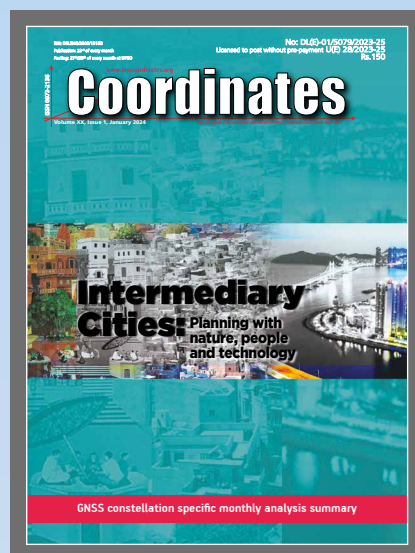
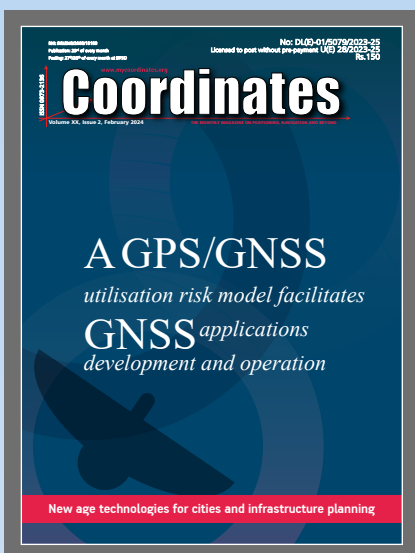
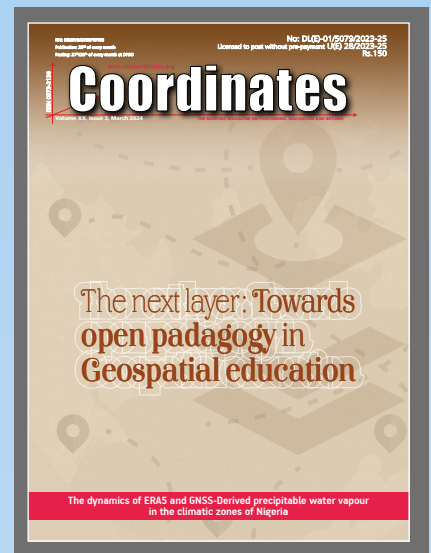
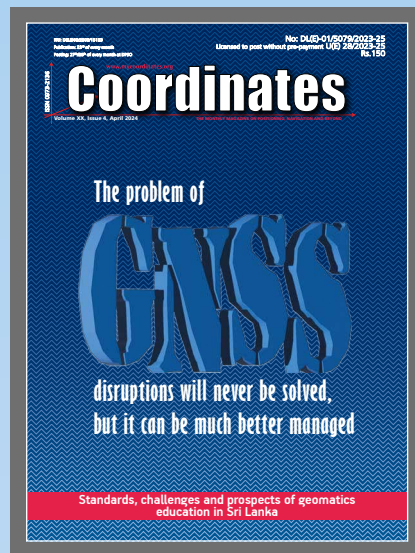
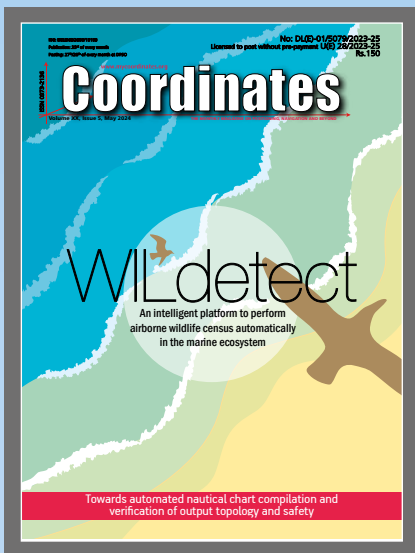
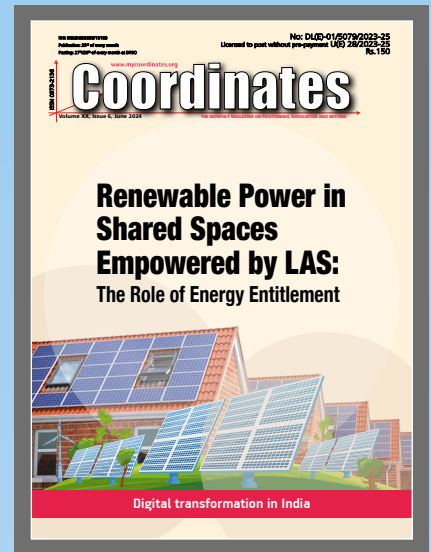
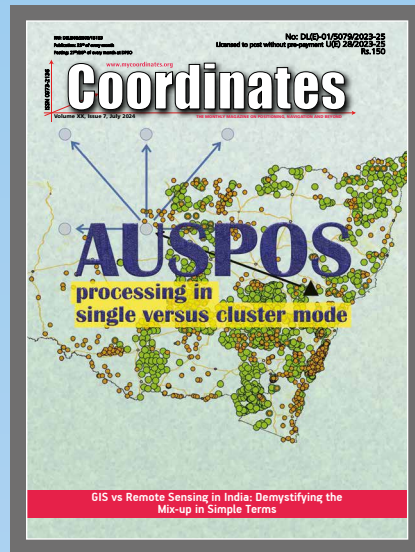
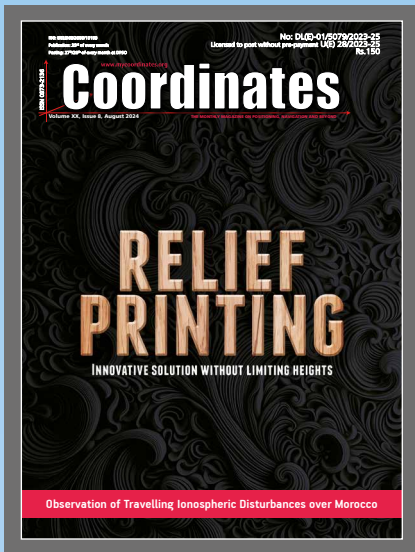
An urban digital twin combatting heat islands and flooding

e-GEOS is Prime Contractor of the consortium commissioned by the European Space Agency (ESA) to develop a digital twin for the simulation of heat island and urban flooding scenarios. The project is called "SURE" (Smart Urban Resilience Enhancement). It will be developed by a consortium led by e-GEOS and composed of Politecnico di Milano (POLIMI), Luxembourg Institute of Science and Technology (LIST) and Stefano BOERI Architetti, with external services provided by the Czech Academy of Sciences, Institute of Computer Science - Department of Complex Systems.

Digital twins are virtual reproductions of the Earth, its environments and the dynamics of territories, allowing people to monitor the health of the Planet. Through simulation scenarios based on satellite data, they can provide information supporting emergency response in the event of extreme weather events. The SURE project integrates multi-platform data from remote and close-range sensing with in-situ information for the development of two digital twins for urban environments, focusing on heat islands and on urban floods. www.telespazio.com

Neo Space Group to acquire UP42 Earth Observation platform

Neo Space Group (NSG), Saudi Arabia has entered into a definitive agreement with Airbus Defence and Space (Airbus) to acquire its UP42 business, a next-generation earth observation digital platform, subject to the satisfaction of customary closing conditions, including required regulatory clearances. UP42, launched by Airbus in 2019 in Berlin, Germany, is a pioneer in streamlining access to and deriving insights from geospatial data via a cloud-based platform. up42.com



“The monthly magazine on Positioning, Navigation and Beyond”
Download your copy of Coordinates at www.mycoordinates.org



Motion & Navigation you can trust

HIGH PERFORMANCE INS/GNSS

- » High-end Technology in the Smallest Package
- » Reliable Navigation and Positioning Everywhere
- » Post-Processing with Qinertia PPK Software



Ekinox Micro

Compact INS for Mission
Critical Applications



Ellipse-D

Smallest Dual-antenna
Multi-band GNSS INS



Ellipse OEM

OEM INS when Size and
Performance Matter